
Article:
Barrett, James orcid.org/0000-0003-2206-2045, Girr, Philipp orcid.org/0000-0002-0036-3181 and Mackinder, Luke orcid.org/0000-0003-1440-3233 (2021) Pyrenoids:CO2-fixing phase separated liquid organelles. Biochimica et biophysica acta-Molecular cell research. 118949. ISSN 0167-4889

https://doi.org/10.1016/j.bbamcr.2021.118949

Pyrenoids: CO_2-fixing phase separated liquid organelles

James Barrett[1]*, Philipp Girr[1]*, Luke C.M. Mackinder[1]

[1]Department of Biology, University of York, York, YO10 5DD, UK
*Equal contribution

ABSTRACT

Pyrenoids are non-membrane bound organelles found in chloroplasts of algae and hornwort plants that can be seen by light-microscopy. Pyrenoids are formed by liquid-liquid phase separation (LLPS) of Rubisco, the primary CO_2 fixing enzyme, with an intrinsically disordered multivalent Rubisco-binding protein. Pyrenoids are the heart of algal and hornwort biophysical CO_2 concentrating mechanisms, which accelerate photosynthesis and mediate about 30% of global carbon fixation. Even though LLPS may underlie the apparent convergent evolution of pyrenoids, our current molecular understanding of pyrenoid formation comes from a single example, the model alga *Chlamydomonas reinhardtii*. In this review, we summarise current knowledge about pyrenoid assembly, regulation and structural organization in *Chlamydomonas* and highlight evidence that LLPS is the general principle underlying pyrenoid formation across algal lineages and hornworts. Detailed understanding of the principles behind pyrenoid assembly, regulation and structural organization within diverse lineages will provide a fundamental understanding of this biogeochemically important organelle and help guide ongoing efforts to engineer pyrenoids into crops to increase photosynthetic performance and yields.

INTRODUCTION

CO_2 concentrating mechanisms accelerate photosynthesis

Photosynthesis is the gateway between inorganic carbon (i.e. CO_2) and organic carbon in the global carbon cycle. It harnesses energy from sunlight to annually reduce ~400 gigatonnes of CO_2 (Net Primary Production; [1]) whilst simultaneously releasing O_2. Given that nearly all carbon fixation is performed by Ribulose-1,5-bisphosphate carboxylase oxygenase (Rubisco), it is puzzling that over its >3.5 billion year existence it has remained slow (catalytic rates typically 8-10 times lower than the median for central metabolic enzymes [2]) and has a relatively poor selectivity for CO_2 over O_2 under current atmospheric concentrations of 0.04% CO_2 and 21% O_2 [3]. These apparent limitations appear to be due to a trade-off between Rubisco's catalytic rate and its specificity for CO_2 over O_2 [4-6], with oxygenation resulting in energetically wasteful photorespiration. To overcome Rubisco's "bottle-neck" photosynthetic organisms have evolved diverse strategies. Many terrestrial plants attain high CO_2 fixation and reduce photorespiration by investing large amounts of resources into Rubisco that is catalytically slow but has a relatively high CO_2/O_2 specificity. This results in Rubisco typically accounting for approximately 25% of soluble protein in plant leaves [7], making it potentially the most abundant enzyme on earth [8, 9]. An alternative strategy evolved by some plants and nearly all aquatic photosynthetic organisms is to operate CO_2 concentrating mechanisms (CCMs) that actively concentrate CO_2 at Rubisco's active site, thus enabling high CO_2 fixation rates with lower amounts of faster, less specific Rubisco.

CCMs can be broadly split into two types: biochemical and biophysical. This review focuses on biophysical CCMs, the dominant CCM type found in aquatic photosynthetic organisms. Biophysical CCMs typically function via the concentration of inorganic carbon in the form of bicarbonate (HCO_3^-) and its subsequent dehydration to CO_2 in a Rubisco rich compartment. This functionality is achieved through out-of-equilibrium carbonate chemistry, pH changes across membranes and the heterogeneous distribution of carbonic anhydrases [10-13]. The slow, uncatalyzed equilibrium of HCO_3^- and CO_2 enables the accumulation of HCO_3^- that has a lower membrane permeability as compared to uncharged species like CO_2; pH determines the HCO_3^-:CO_2 ratio, with HCO_3^- ~100 times more abundant than CO_2 at pH 8, thus enabling HCO_3^- concentration at higher pH or CO_2 release at lower pH; and the specific spatial distribution of carbonic anhydrases enables the rapid equilibrium of HCO_3^- and CO_2 to drive HCO_3^- formation for concentration or CO_2 release for Rubisco fixation.

Biophysical CCMs found in oxygenic phototrophs can be generally split into two types: carboxysome based CCMs found in prokaryotic cyanobacteria, and pyrenoid based CCMs found in eukaryotic algae and some non-vascular plants (i.e. most hornwort species). Cyanobacterial carboxysomes are icosahedral 100+ megadalton protein assemblies where densely aggregated Rubisco is encapsulated in a protein shell with a typical diameter of 150-200 nm [14]. HCO_3^- concentrated in the cyanobacterial cytosol diffuses into the carboxysome through hexameric shell proteins where it is dehydrated to CO_2 via carbonic anhydrase for fixation by Rubisco. Algal pyrenoids are also Rubisco assemblies, but they are much larger than carboxysomes (~1-2 μm diameter), are dynamic in size by growing and shrinking in response to CO_2 and light, lack a proteinaceous shell, and are typically traversed by membranes that are continuous with the thylakoid network [15]. These characteristic membrane traversions are thought to be the primary source of inorganic carbon delivery, where HCO_3^- is converted to CO_2 in the acidic lumen, creating a “point source” of CO_2 within the pyrenoid.

Understanding CCMs at the molecular level across diverse species is critical for understanding biotic contributions to the global carbon cycle and for providing engineering solutions to address human driven pressures on our planet. CCM driven cyanobacterial and algal photosynthesis accounts for approximately half of global net primary production [1] and plays a critical role in the buffering of anthropogenic CO_2-driven global warming through driving the “biological pump” that moves carbon from the upper ocean to the deep ocean for long-term storage [16]. In addition, modelling suggests that engineering crops with CCMs may significantly increase photosynthetic performance. If these improvements translate to yield the engineering of a CCM into crops such as rice, wheat and soya could increase yields by up to 60% [17], a significant step towards the goal of the predicted ~85% increases required to feed the global population in 2050 [18].

Box 1: General properties of LLPS systems

Liquid-liquid phase separation (LLPS) is the process by which a homogeneous solution reversibly demixes to form a dense phase that is distinguished from a coexisting dilute phase. The solution composition, concentration and conditions (pH, temperature etc.) define a phase diagram for demixing that is bounded by a coexistence line (also known as the binodal) that determines the one- and two-phase states (Figure 1).

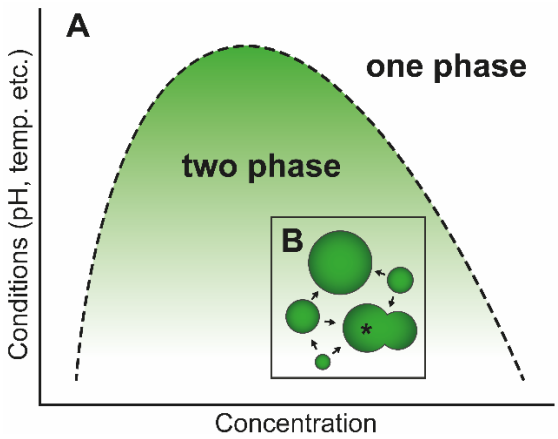

Figure 1. Phase diagrams explain LLPS. A) A phase diagram determines a one- and two-phase state of the system, where the two-phase state consists of droplets distinguished from the coexisting dilute phase. Changes in solution conditions that affect interaction strength (y) and concentration of components (x) alter the phase state of the system relative to the coexistence line (black dashed). **B)** Schematic of droplet growth where Ostwald ripening is shown with arrows that indicate the trafficking of solute from smaller to larger droplets. Asterisk indicates coalescence of two adjacent demixed droplets.

In biology, LLPS is thought to give rise to an array of membraneless bodies [19] that provide spatiotemporal control over diverse cellular processes [20], by concentrating particular protein and nucleic acid species relative to the bulk phase [21], whilst permitting a rapidly diffusing biochemical environment [22]. Although membraneless bodies were described as early as 1803 [23], their liquid-like properties were demonstrated much more recently. Brangwynne et al. [24] reported fusion, dripping, fission and internal/external rearrangement of spherical P granules over second timescales in 2009. These observations hold true for many biomolecular condensates, where growth can occur by Ostwald ripening (growth of larger droplets at the expense of smaller droplets to reduce surface tension energetic penalty; Figure 1B) and elastic ripening (transport of solute down a stiffness gradient) in addition to coalescence (Figure 1B, asterisk) [25, 26]. It should be highlighted that many systems have been classified as LLPS based on these qualitative descriptions, though other mechanisms of biomolecular condensate assembly are possible, and quantitative descriptors are required for their distinction [27].

Given their liquid-like nature, it is postulated that membraneless bodies can respond more rapidly to environmental cues than membrane-bound compartments [28], and as such are implicated in many transitory processes across a vast array of cellular contexts. Their composition is often accordingly vast [29], and accompanied by an array of underpinning interactions, including electrostatic, π-π, cation-π, hydrophobic associations and hydrogen bonds between subsumed components [30]. These interactions are often weak in nature and high in valency (number of binding sites on a binding partner) to facilitate formation of a network of interactions, required for phase separation [31]. This network forms homotypically, in simple coacervation, or between multiple protein species in complex coacervation [19]. Across these coacervation mechanisms, multivalency is provided by a range of associating sequence and structural features, comprising folded and/or unfolded domains, that can be loosely termed ‘stickers’. Variegating these stickers, are regions of structure or sequence that are termed ‘spacers’ [32]. Although often not directly involved in coacervation interactions, spacer presence and composition has marked effects on condensate properties, dependent

on their solvation properties, but little effect on phase separation driving forces has been demonstrated [33]. Changes in valency, concentration and affinity of stickers sharply determines phase separation thresholds [21] and coacervate composition [34]. These changes often occur rapidly, through sharp transitions that can be influenced by a host of cellular factors, both globally (pH, temperature and ionic strength - see Dignon et al. [30] for review) and targeted (including methylation, phosphorylation, acetylation, SUMOylation - see Owen and Shewmaker [35]), that account for condensate transiency.

Despite experiencing rapid transitions in response to relatively minute changes, biomolecular condensates can be stable throughout generational lifetimes (e.g. the *Chlamydomonas reinhardtii* pyrenoid that is inherited and maintained through multiple cell division events [36]), whilst retaining their liquid-like properties. Owing to their liquid nature, condensate morphology can be reversibly deformed, by wetting (adherence to solid surfaces due to intermolecular interactions) [24], disruption [37] or compositional effects [38], commonly observed in the cellular environment. Surface tension underpins this behaviour [39], and is affected by coacervate component interaction strength and valency [38]. A range of viscosity is also observed across coacervates and their lifetimes, and has been implicated in their functionality [40]. The maturation of condensates to more solid states has been proposed to occur *in vivo* [22], mirroring the effect of gelation (transition towards a less dynamic structure underpinned by interaction strength increase) that influences droplet dynamics *in vitro* [41]. The mechanistic implications of these macroscopic properties are relatively unexplored [30, 31], but are likely central to condensate activity regulation and physical resilience. Accordingly, microscopic perturbations that alter macroscopic properties are functionally intertwined. The movement of species within biomolecular condensates is influenced by both macroscopic and microscopic properties. The porosity of the primary scaffold components that constitute condensates determines the relative mobility of their subsumed components in a size-dependent manner [22], referred to as the mesh-size, that is dependent on the extent of physical cross links [31]. Microscopically, the interaction of diffusing species with the biomolecular scaffold will also influence their mobility.

Pyrenoid and carboxysome assembly is driven by disordered, multivalent Rubisco binding proteins

In recent years, it has become clear that aggregation of Rubisco by disordered, multivalent binding proteins is a required precursor for formation of pyrenoids in the model alga *Chlamydomonas reinhardtii* (*Chlamydomonas* from here on) and carboxysomes in model cyanobacteria and proteobacteria [36, 42-44]. There are two types of carboxysomes, α and β, that appear to have evolved independently. Nearly all of their components have counterparts across the carboxysome types, including a “linker” that interacts multivalently with Rubisco, enabling liquid-liquid phase separation (LLPS) through complex coacervation (see Box 1 for an introduction to general properties of LLPS systems) [14]. In the α-carboxysome, CsoS2 multivalently binds Rubisco driving carboxysome assembly whilst in the β-carboxysome CcmM performs an analogous role. In both cases deletion of CsoS2 or CcmM abrogates carboxysome assembly leading to a high-CO_2 requiring phenotype – the characteristic signature of a non-functional CCM [45, 46]. Demixing occurs when truncated CsoS2 or CcmM, containing only the multivalent Rubisco interacting domains, are mixed with the corresponding Rubisco *in vitro* [43, 47]. It is postulated that Rubisco condensation may play a key role in

carboxysome assembly for both carboxysome types. However, the lack of Rubisco mobility within β-carboxysomes suggests that the role of LLPS may be limited to assembly [48].

In contrast to the two evolutionary origins of carboxysomes, and the clear conservation of carboxysome components across species [49], pyrenoid evolution appears to be far more complex. Pyrenoids are thought to have evolved multiple times [15, 50] and there is apparent absence of conserved structural components across diverse algal lineages (see Box 2 for an overview of algal diversity) [15, 51]. Nearly all of our data on pyrenoid formation is based on *Chlamydomonas*, where the multivalent disordered protein EPYC1 (Essential Pyrenoid Component 1, formerly LCI5), causes the aggregation of Rubisco through complex coacervation [36, 44, 51]. However, EPYC1 homologs are not found outside of closely related green algae, making drawing conclusions of pyrenoid assembly across algal lineages difficult. This review aims to integrate our current knowledge of the algal pyrenoid with the rapidly advancing field of biological LLPS in a drive to identify key unanswered questions that can guide our understanding of pyrenoid form and function across diverse algae to give insights into this biogeochemically important organelle and help guide engineering efforts into crops to increase yields.

Box 2: Pyrenoid occurrence and overview of algal diversity

Pyrenoids occur in all algal lineages and most hornworts (Figure 2) but are missing in all other land plants (liverworts, mosses, and vascular plants). The high diversity of algae, their long evolutionary history and pyrenoid apparent loss and reappearance means that pyrenoids possibly have tens to hundreds of evolutionary origins [50]. Algae is a polyphyletic term for mostly aquatic photosynthetic eukaryotes, which includes over 70,000 different extant species [52]. The phylogeny of algae is controversial. For this review, we group algae into seven clades according to their chloroplast ancestry [53]. The 1st clade, Archaeplastida, which contains glaucophytes, rhodophytes (red algae) and green algae (core chlorophytes, charophytes and prasinophytes) (and land plants), acquired their chloroplasts through a primary endosymbiosis of a cyanobacterium. All other algal clades inherited their chloroplasts through secondary or even tertiary endosymbiotic events. The 2nd clade, excavates, which contains only one photosynthetic group (euglenids), and the 3rd clade, rhizaria, only containing photosynthetic chlorarachniophytes, inherited their chloroplasts through a secondary endosymbiosis of a green alga. The 4th clade, stramenopiles (containing xanthophytes, chrysophytes, phaeophytes and bacilliarophytes/diatoms) inherited their chloroplasts through a secondary endosymbiosis of a red alga. In the 5th clade, alveolates (containing dinoflagellates), chloroplast inheritance is complex with species having secondary or tertiary plastids originating from both red and green algal lineages. Algae belonging to clades 3, 4 and 5 are often summarised to the TSAR supergroup (Figure 2). The 6th clade (containing haptophytes) and the 7th clade (containing cryptophytes) both inherited their chloroplasts through a secondary endosymbiosis of a red alga.

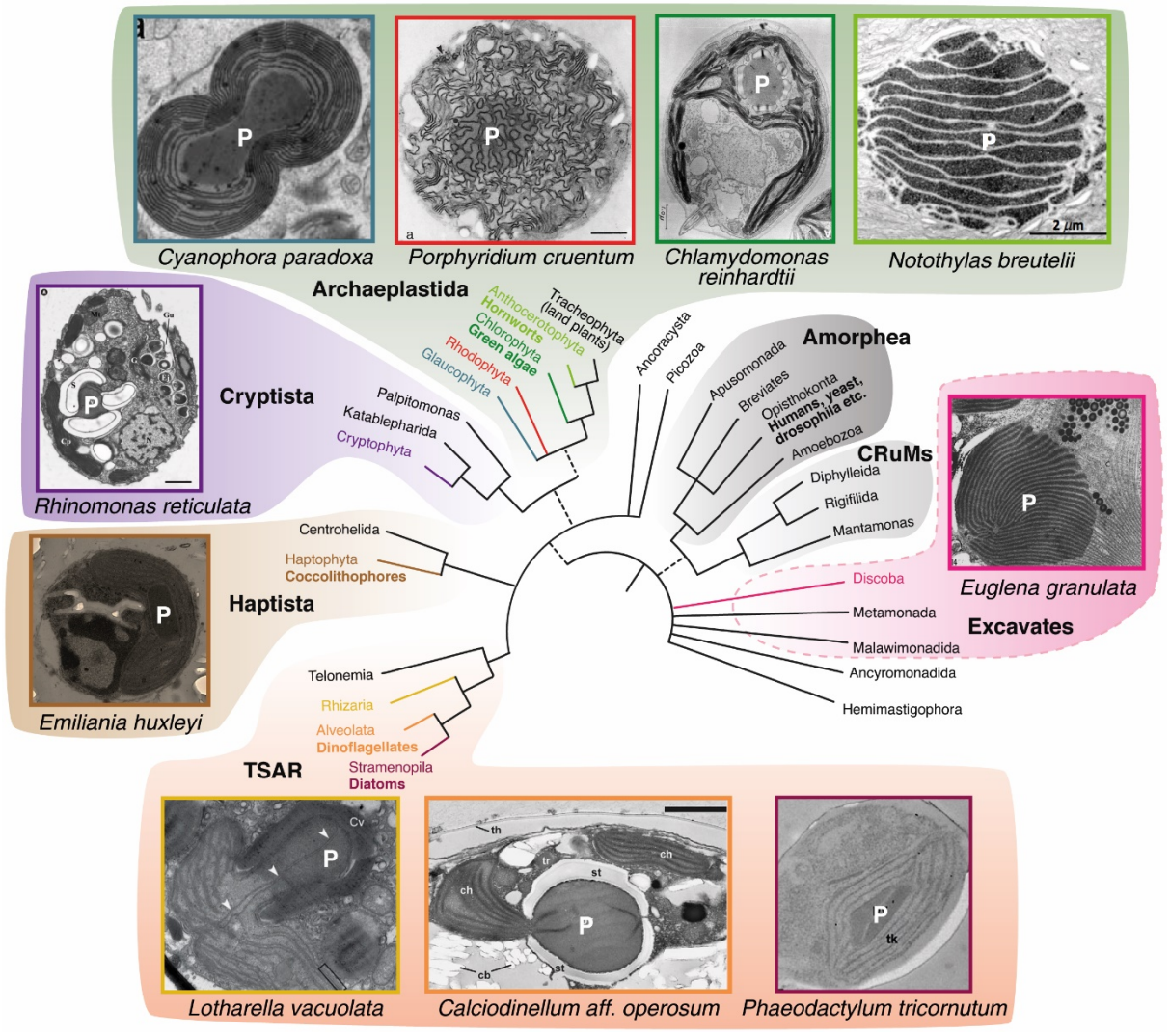

Figure 2. Pyrenoid containing algae are polyphyletic and found across the eukaryotic tree of life. Tree is based on Burki et al. [53]. Dashed lines indicate uncertainty about the monophyletic nature of these groups. Transmission electron microscope image descriptions (clockwise from top left): A dividing pyrenoid (also known as central body) of the glaucophyte *Cyanophora paradoxa* [54]. *Porphyridium cruentum* with thylakoid membranes stained dark via photooxidation of 3,3'-diaminobenzidine.4HCl (DAB) that depicts Photosystem I activity [55]. The model green alga *Chlamydomonas reinhardtii* [56]. *Notothylas breutelii* [57]. *Euglena granulata* [58]. The model diatom *Phaeodactylum tricornutum* [59]. The dinoflagellate *Calciodinellum* aff. *operosum* [60]. *Lotharella vacuolata* [61]. The abundant biogeochemically important calcifying coccolithophore *Emiliania huxleyi* (author's collection). *Rhinomonas reticulata* var. *atrorosea* [62]. P indicates pyrenoid.

A brief history of the pyrenoid

The relatively large size and high density of pyrenoids make them easy to see via light microscopy, with descriptions in algae referring to the pyrenoid from 1803 (Figure 3; [23]) and the first reports of pyrenoids in hornworts from 1885 [63]. As a result, pyrenoids may be the first LLPS organelles to be described, with the nucleolus described later in 1835 [64]. The term pyrenoid was coined in 1882 [65] and its presence and ultrastructural variation across

evolutionarily-diverse algae was described throughout the mid-1900s by the increased use of TEM imaging, which also allowed characterization of the pyrenoid ultrastructure. From early TEM images, it was assumed that the pyrenoid matrix, depending on the species, was either crystalline or amorphous. In the 1970s Rubisco was shown to be a major constituent by enzymatic characterization of purified pyrenoids and analysis of Rubisco knock-out lines [66-69], which was later confirmed by immunocytochemistry [70, 71]. The association between pyrenoid presence and efficient CCM function was first made in the 1990s, when experimental observations showed that pyrenoid containing algae have an efficient CCM, with CCM induction concurrent with biochemical and structural changes to the pyrenoid, whereas algae lacking a pyrenoid either lack a CCM or have a reduced ability to concentrate CO_2 [72-75]. The discovery that EPYC1 linked Rubisco to form the pyrenoid was made in 2016 [51] and its LLPS nature identified in 2017 [36].

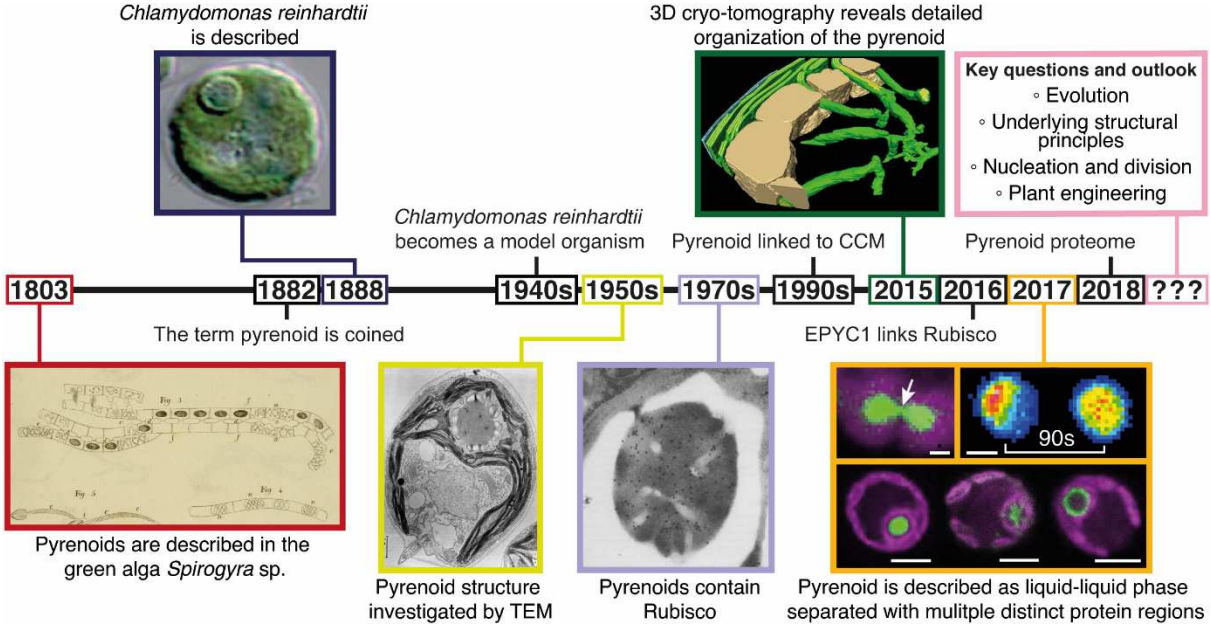

Figure 3. A brief history of the pyrenoid. Pyrenoids were first described in the green alga *Spirogyra* by Jean-Pierre Vaucher in 1803. The original drawings by Vaucher display one ribbon-like chloroplast per cell that contains multiple spherical pyrenoids [23]. In 1882, the term pyrenoid (Greek *pyrene*, stone kernel-like) was coined by Friedrich Schmitz, who observed pyrenoids in several algae species [65]. Six years later, in 1888 the model alga *Chlamydomonas reinhardtii* was first described by Pierre Augustin Dangeard [76]. *Chlamydomonas*, which is the central model for pyrenoid research, has one pyrenoid per cell that is visible in light microscopy (light microscopy image by Moritz Meyer [77]). In the 1940s, *Chlamydomonas* entered into research labs and over time became an essential model system [78]. The use of TEM to image algae from the early 1950s onward made details of the pyrenoid ultrastructure with matrix, traversing thylakoids and starch sheath visible (TEM image of *Chlamydomonas* by Ohad et al. [56]). From the 1970s onward, it became clear that the pyrenoid contains most of the cell's Rubisco, which later in 1980s was incontrovertibly proved by immunogold labelling (TEM image of immunogold-labelled Rubisco (black dots) in *Chlamydomonas* by Lacoste-Royal et al. [70]). The first associations of the pyrenoid with the CCM were made in the 1990s. In 2015, the 3D structure of the *Chlamydomonas* pyrenoid was resolved by cryo-EM tomography (reconstruction of the pyrenoid (thylakoid tubules in green, starch sheath in beige, matrix is not displayed) by Engel et al. [79]). EPYC1 and its function as a Rubisco linker in the *Chlamydomonas* pyrenoid was

discovered in 2016 [51]. In 2017 it was shown that the pyrenoid is formed by liquid-liquid phase separation (top left, the pyrenoid divides via fission; top right, fluorescent recovery after photobleaching shows that Rubisco undergoes internal mixing over second timescales in the pyrenoid) [36] and multiple distinct protein regions were described, including the pyrenoid matrix (left, Rubisco), pyrenoid tubules (middle, PSAH) and starch sheath (right, LCI9) [80] (fluorescence microscopy images (magenta: chlorophyll, green: labelled protein). Zhan et al. [81] reported a pyrenoid proteome in 2018.

STRUCTURE AND FUNCTION OF THE *CHLAMYDOMONAS* PYRENOID

The functionality of pyrenoids to concentrate CO_2 at Rubisco's active site to enhance carboxylation requires structural features in addition to the formation of the pyrenoid matrix through Rubisco-EPYC1 condensation. Central to CO_2 concentration and pyrenoid function is the shuttling of inorganic carbon through the subcellular environment to Rubisco within the pyrenoid. The spatial segregation of a carbonic anhydrase within the pyrenoid is essential for catalysing the subsequent dehydration of inorganic carbon (in the form of HCO_3^-) to CO_2, allowing release for carboxylation by Rubisco in the pyrenoid matrix. As discussed above, these characteristics are considered basal for the function of biophysical CCMs and are thus expected to be conserved across pyrenoid-based CCMs, despite ultrastructural variations (Figures 2 and 6).

Although ultrastructural information is available for a wealth of species across diverse lineages (see later section: *Pyrenoid structural diversity across different algal lineages*), our most complete insights relating to pyrenoid form and function are for *Chlamydomonas.* Detailed three-dimensional structural information of the pyrenoid obtained by ion beam milling cryo-electron tomography (cryo-ET; [79]), quick freeze deep-etch electron microscopy (QFDEEM; [51]) and pyrenoid protein fluorescence localization [80], have significantly enhanced our understanding of pyrenoid architecture (Figures 3 and 4). Further, proteomics of pyrenoid-enriched fractions have revealed the complex composition of the pyrenoid, containing at least 190 different proteins, many of which remain uncharacterized [51, 81]. An integrated localization and interaction study also indicated a large number of pyrenoid components (89), many of which have been localized at sub-pyrenoid resolution [80]. Although many different proteins have been localized to the pyrenoid, proteomic analysis shows the pyrenoid matrix consists mainly of Rubisco molecules (~600 μM matrix concentration; [36]) and the intrinsically disordered linker protein EPYC1, that is essential for condensation of Rubisco to form the pyrenoid matrix (Figure 4B) [36, 51]. Here, Rubisco functions within the Calvin-Benson-Bassham (CBB) cycle, with strong evidence supporting that it is the only CBB enzyme partitioned within the pyrenoid [82].

In addition to the pyrenoid matrix, traversing thylakoid tubules form a characteristic star-shaped network within the pyrenoid. *In situ* cryo-ET in *Chlamydomonas* has revealed the intriguing complexity of thylakoid membrane organization and structural changes as it enters the pyrenoid matrix. Thylakoid membranes outside of the pyrenoid are organized in multiple parallel stacked membrane layers [83], which drastically change as they enter the pyrenoid matrix through fenestrations in the transient stromal starch sheath. The membrane layers merge into cylindrical structures, termed pyrenoid tubules, that advance through the pyrenoid matrix and converge in the centre of the pyrenoid, forming an interconnected network of smaller, shorter tubules [79]. Within pyrenoid tubules, minitubules form luminal conduits between the chloroplast stroma and the pyrenoid matrix and based on their diameter (~3-4 nm at matrix opening) have been proposed to facilitate exchange of ATP and CBB metabolites

(incoming Ribulose 1,5 bisphosphate (RuBP) and outgoing 3-phosphoglycerate (3PGA)) but not proteins (Figure 4C) [51, 79, 82]. The wider lumen of the pyrenoid tubules is continuous with the thylakoid lumen and is postulated to transport HCO_3^- towards the centre of the pyrenoid, following channelling from the chloroplast stroma into the thylakoid lumen through bestrophin-like channels [84]. Central to CO_2 delivery is the carbonic anhydrase, CAH3, that catalyses the dehydration of HCO_3^- to CO_2 in the acidic lumen of the pyrenoid tubules. This process enables CO_2 diffusion across the tubule membrane into the pyrenoid matrix for fixation by Rubisco (Figure 4D). CAH3 has been localized to the pyrenoid tubules and a *cah3* mutant has a defective CCM, despite accumulating inorganic carbon at higher concentrations than wild-type [11, 85-87]. There is strong evidence that the pyrenoid tubules also differ in their protein composition from the rest of the thylakoid membrane. Immunogold labelling and photosystem (PS) I and PSII activity assays suggested that the pyrenoid tubules contain active PSI but not PSII [88]. However, recent fluorescent protein tagging of several photosystem proteins revealed that subunits of both photosystems are present in the tubules, indicating that partially-assembled or inactive PSII may be present [80]. Strikingly, some PSI subunits e.g. PSAH are even enriched in the tubules. The functional implications of these depletion/enrichment patterns are yet to be experimentally shown but could be related to reducing photorespiration by minimizing O_2 release within the pyrenoid through photosynthetic H_2O splitting at PSII reaction centres. However, collectively, these observations highlight the importance of membrane traversions in the metabolic fluxes of the pyrenoid and suggest an important role in its photosynthetic operation.

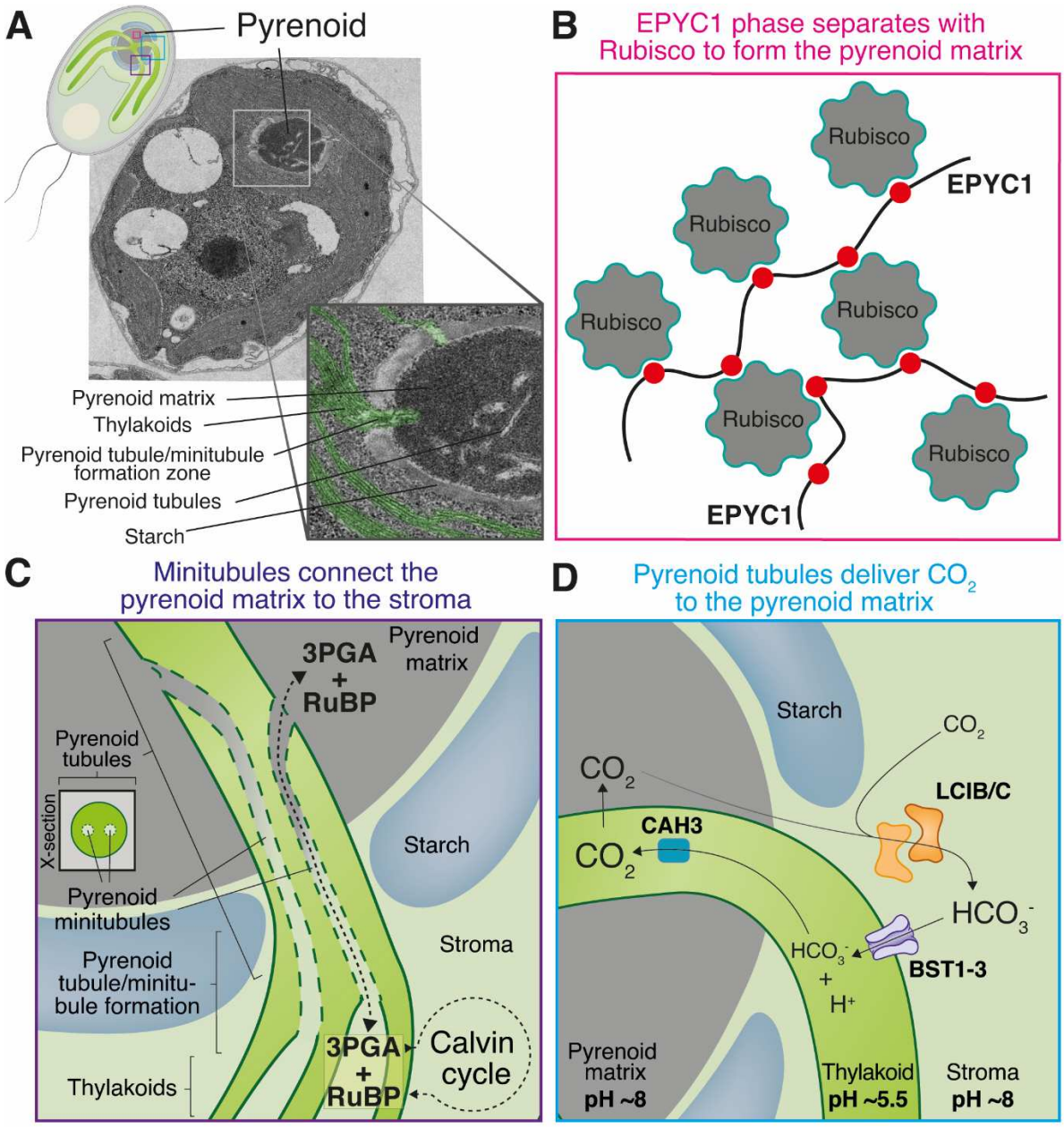

Figure 4. The *Chlamydomonas* pyrenoid is at the heart of the CO_2 concentrating mechanism and enables efficient CO_2 fixation. A) TEM image of *Chlamydomonas reinhardtii* grown in light and under air levels of CO_2 where a complete pyrenoid is assembled. Zoom highlights key structural parts of the pyrenoid. Thylakoids false coloured green for clarity. Top left diagram is for orientation of panels B-D. **B)** The pyrenoid matrix is predominantly composed of Rubisco-EPYC1 condensate. Multiple Rubisco binding regions on EPYC1 enable complex coacervation with the Rubisco holoenzyme which is a hexadecameric assembly of 8 large and 8 small subunits. **C)** As thylakoids enter the pyrenoid they form pyrenoid tubules. Minitubules (dashed lines) form within the pyrenoid tubules and connect the pyrenoid matrix to the stroma. They are postulated to enable the large flux of metabolites in and out of the pyrenoid. Inset: cross-section (X-section) of minitubules within a pyrenoid tubule. **D)** Pyrenoid tubules are proposed to deliver CO_2 to Rubisco in the pyrenoid matrix. Current data supports that HCO_3^- enters from the stroma into the thylakoid lumen via bestrophin-like channels. In the acidic lumen HCO_3^- is converted to CO_2 via CAH3 and subsequently diffuses into the pyrenoid matrix. LCIB/LCIC is proposed to convert stromal CO_2 to HCO_3^- via active CO_2 uptake and CO_2 recapture from the pyrenoid. Minitubules are not shown for clarity.

The *Chlamydomonas* pyrenoid is surrounded by a sheath that is composed of several starch plates. The starch sheath develops rapidly under limiting CO_2 concentrations [89] and has been proposed to act as a diffusion barrier to reduce the loss of CO_2, that diffuses readily between the stroma and matrix [73]. Although it has been suggested that the absence of the starch sheath does not affect photosynthetic productivity [90], recent studies indicate a correctly formed starch sheath is required for normal pyrenoid formation and the operation of an efficient CCM [42, 91]. In addition to starch, the sheath also contains several proteins. These proteins appear to be distributed uniformly over the starch plates, or localized in distinct puncta or meshes in close proximity to the starch plates [80]. The functional implications of these different distribution patterns remain unclear, but their positioning appears to be important for CCM function [91]. A subset of proteins that localize in a plate-like pattern are predicted to function as starch-branching enzymes, whereas the mesh distributed proteins appear to fill the gaps between the starch plates, indicating a potential structural function [80]. Recently, a predicted starch-binding Rubisco-interacting protein, SAGA1 (StArch Granules Abnormal 1), that localizes to distinct puncta at the pyrenoid matrix/starch interface was shown to affect pyrenoid number and sheath morphology [42]. Interestingly, the two carbonic anhydrase homologs, LCIB and LCIC, that are recruited to the pyrenoid in very low CO_2 concentrations (<0.02% CO_2) are also localized in distinct puncta but on the external surface of the starch sheath [80, 92], where they are expected to minimize the loss of CO_2 from the pyrenoid by converting emanating CO_2 back to HCO_3^-, that can be readily concentrated again (Figure 4D) [93]. LCIB homologs show *in vitro* carbonic anhydrase activity, however this could not be demonstrated for the *Chlamydomonas* LCIB/LCIC proteins [94], potentially indicating the absence of critical regulatory subunits or that activity requires specific cellular conditions.

EPYC1 links Rubisco to form the pyrenoid matrix

In *Chlamydomonas*, the abundant, low CO_2-induced linker protein, EPYC1, underpins the functional phase separation of Rubisco to form the pyrenoid [44, 51]. In mutants depleted of EPYC1, Rubisco fails to aggregate and is dispersed in the chloroplast [51], resulting in a deficient CCM [51]. EPYC1 is a low complexity, largely disordered ~35 kDa protein, consisting of five near-identical repeats [44, 51, 95]. Each ~60 amino acid repeat contains a predicted α-helix, and significant charge patterning [44, 51]. The high isoelectric point (pI) of EPYC1 (11.7) establishes a net positive charge of the unmodified protein in the slightly basic pyrenoid matrix (pH ~7-8.5), in both photosynthetic and non-photosynthetic conditions [36, 96]. As described above, *in vitro* demixing assays have demonstrated that LLPS of Rubisco by EPYC1 occurs via complex coacervation, in which both components are required [44]. In line with general LLPS principles, demixing was also demonstrated to require multivalent interactions between the Rubisco holoenzyme and EPYC1 [29, 97].

Prior to EPYC1 discovery and functional characterization, Meyer et al. [98] demonstrated that the sequence composition of the surface-exposed α-helices of the Rubisco Small Subunit (SSU) was conditional for *Chlamydomonas* pyrenoid formation. Wunder et al. [44] confirmed the importance of this interface for *in vitro* demixing and suggested the association could be dominated by charge interactions between negative patches of the SSU α-helices and regions of patterned positive charge in EPYC1. Yeast two-hybrid (Y2H) data confirmed the SSU α-helices are necessary for interaction with EPYC1, and that other SSU features enhance this interaction [97]. In line with previous predictions [51], it was later demonstrated that EPYC1's interaction with Rubisco is enhanced by its repeating helical regions [97]. More recently, single particle cryo-electron microscopy of a complex of Rubisco and a 24 amino acid EPYC1 peptide containing the helical region has outlined the structural

basis for this interaction, revealing a primarily electrostatic and hydrophobic interface [95]. The peptide was bound to each of the SSUs of Rubisco, indicating the holoenzyme can bind one of EPYC1's five helical regions up to 8 times. In the same study, mutation of EPYC1 interface residues decreased demixing of Rubisco *in vitro* and Rubisco substitutions at the interface prevented pyrenoid formation *in vivo*, confirming the role of this low affinity interaction in condensation of Rubisco. It is proposed that consecutive binding regions of the full length EPYC1 peptide can facilitate the low affinity, multivalent interactions with multiple Rubisco molecules required for condensation into the pyrenoid matrix. Key to this model, is the ability for the unstructured region between two adjacent helical regions to span the distance between Rubisco holoenzymes in the pyrenoid. *In-situ* cryo-ET data indicates a median distance of ~4 nm between EPYC1 binding sites on adjacent holoenzymes [79, 95]. The ~40 amino acid unstructured regions between the 5 binding regions of EPYC1 are proposed to facilitate the spanning of this distance, with wormlike chain models indicating a minimal energetic cost (< 3 k_bT) for stretching [95].

EPYC1 displays functional similarity to CsoS2 and CcmM in cyanobacteria [43, 46, 47]. Both EPYC1 and CsoS2 utilise helical regions to contact Rubisco, whereas CcmM utilises a Rubisco SSU-like globular domain. Although all three Rubisco condensation events appear to be underpinned by a similar multivalent mechanism, the sequences of the Rubisco-interacting regions of CsoS2 and CcmM bear no homology to each other nor EPYC1, suggesting a convergent evolutionary mechanism. CsoS2 and CcmM concurrently contact both the large and small subunits of the morphologically similar form I Rubisco holoenzyme (L_8S_8) in the cyanobacterium *Synechococcus elongatus* and the chemoautotrophic proteobacterium *Halothiobacillus neapolitanus* respectively [43, 47]. It is postulated that the concurrent binding of CsoS2 and CcmM to both the Rubisco large and small subunits results in only fully assembled and functional Rubisco holoenzymes being incorporated into the carboxysome [43, 47]. Current data suggests that EPYC1 may exclusively contact the small subunit [95]. Additionally, whereas CsoS2 and CcmM facilitate aggregation using only a portion of their full-length sequence, EPYC1 appears to dedicate its full length to multivalent interactions with Rubisco [43, 47]. Although it is expected that linker proteins facilitate phase separation of other pyrenoids [99], the lack of obvious EPYC1 homologs suggests that analogous linker proteins will display a range of sequence characteristics across pyrenoid lineages, especially outside of the Archaeplastida (form IB Rubisco), where Rubisco forms are variant (dinoflagellates/alveolata [form II], all other clades [form ID]). Predictions based on characterized linkers, suggest that analogous proteins contain: a) regions of disorder that are continuous and cover part, or all of the protein sequence; b) repeat motifs within this disordered region that will interact with Rubisco using localized structure; c) patterning of charged residues throughout the full-length protein; and d) low complexity amino acid sequences. Mackinder et al. [51] predicted the presence of analogous proteins in four other species using a search framework based on some of these constraints, but these are yet to be experimentally validated. These observations, alongside data from green algae that pyrenoid presence is not determined by SSU sequence [100], certainly suggest that the presence of analogous linker proteins is probably widely determinant of pyrenoid formation across lineages.

Although considerable progress has been made to characterize the EPYC1-Rubisco interaction, several questions remain outstanding. The average fraction of bound sites for both EPYC1 and Rubisco are uncharacterized (Figure 5A). In addition, although EPYC1's helical interaction is well defined, the behaviour of the flexible regions between the helices are largely unassessed. In other condensates, the length and interactions of these flexible regions have

been demonstrated to affect assembly [33], and should be considered in future studies of pyrenoid dynamics.

A Rubisco-binding motif targets proteins to the pyrenoid and may guide pyrenoid assembly

Recent work has proposed a framework for pyrenoid assembly in *Chlamydomonas* [101]. Multiple pyrenoid localized proteins were shown to contain a conserved Rubisco-binding motif (RBM). This RBM is repeated five times in EPYC1 and two or more times, including at the C-terminal, in other confirmed pyrenoid localised proteins. The EPYC1 RBM forms part of the α-helix that directly binds Rubisco [95]. The RBM is found in proteins with diverse structural features including predicted transmembrane domains and predicted starch binding domains. Two proteins that contain both RBMs and transmembrane domains (termed Rubisco binding membrane proteins 1 and 2 [RBMP1/2]) specifically localised to the pyrenoid tubules. Whilst two proteins containing RBMs and starch binding motifs, SAGA1/2, localized to the pyrenoid matrix/starch interface. Fusion of the motif to both non-pyrenoid localised stromal and transmembrane thylakoid proteins resulted in targeting to the pyrenoid matrix and pyrenoid tubules respectively. An elegant assembly mechanism is suggested, in which RBMP1/2 tether the Rubisco matrix to the pyrenoid tubules and that SAGA1/2 tether the starch sheath to the matrix [101]. However, characterization of RBMP1/2 deletion mutants has yet to be completed and there is contradictory evidence supporting the role of SAGA1 as purely a Rubisco matrix/starch tether, with a SAGA1 mutant having a severely disrupted CCM, abnormal starch and multiple pyrenoids [42]. It might be expected that a mutant where starch tethering is absent would have a phenotype in line with a starchless mutant, which retains a canonical single pyrenoid and has only a slightly defective CCM [91]. Further work is required to understand if RBMs are purely for pyrenoid structural assembly (as in matrix assembly via EPYC1) or whether it is a mechanism to target functional proteins to specific sub-pyrenoid regions (Figure 5A).

Pyrenoid assembly around membranes and pyrenoid tubule formation

Pyrenoids are one of two identified LLPS organelles that are crossed by a membrane system. The others are sponge bodies, organelles so far only observed in germline cells of *Drosophila melanogaster* and *Caenorhabditis elegans* [102]. Sponge bodies are ribonucleoprotein granules found in the cytoplasm, which are crossed by multiple ER cisternae [103, 104]. The function of sponge bodies remains unclear. Even though membrane traversion of LLPS organelles is rarely observed so far, several interactions between LLPS organelles and membranes have been reported, where the membraneless organelle is directly attached to a membrane. These include: T cell and other receptors [105, 106]; nuclear pore complexes [107]; ribonucleoprotein granules such as P-bodies, stress granules and TIS granules that interact with the ER [108, 109]; the yeast pre-autophagosomal structure that is attached to the vacuole [110]; and the protein synapsin, which can phase separate and recruit lipid vesicles to the droplets *in vitro* [111]. This broad range of reported interactions between membraneless organelles and membranes imply that these interactions are quite common and play a role in various biological processes. For some LLPS organelles that are attached to a membrane, there is evidence that proteins often function as tethers. For instance, the pre-autophagosomal structure of yeast is tethered to the vacuole via protein-protein interactions between several intrinsically unfolded proteins of pre-autophagosomal structure and tonoplast membrane proteins [110]. This would support the role of RBMP1/2, or other transmembrane containing Rubisco interacting proteins, functioning as pyrenoid matrix membrane tethers.

However, other pyrenoid tubule membrane attachment mechanisms are feasible, including the recently demonstrated sensing and direct binding to curved membranes of intrinsically disordered region containing proteins [112, 113] or interactions between pyrenoid proteins and the presumably unique lipid bilayer properties of the pyrenoid tubules.

Whereas some progress is being made on pyrenoid matrix interactions with thylakoid membranes, we know little about the thylakoid tubules within the pyrenoid. The thylakoid membrane in photosynthetic organisms, from which the tubules derive, differs in several respects from other membrane systems. It has an unusual lipid composition and consists of almost 80% uncharged galactolipids, ~10% anionic sulpholipids and ~10% anionic phospholipid [114]. Due to a high content of hexagonal phase forming lipids (~60% of the total lipid), the thylakoid membrane is highly curved. There is no data on the lipid content of pyrenoid tubules versus the bulk thylakoid membranes, although the typical further increased curvature of pyrenoid tubules could result in specific lipid partitioning. Moreover, the thylakoid membrane has a high protein content, with about 70% of the membrane surface occupied by proteins in land plants [115]. The proteins are unevenly distributed over the thylakoid membrane, with some proteins enriched in certain regions of the membrane, while depleted in others [83, 116]. Specifically, the two photosystems (PS) are heterogeneously distributed, with certain regions where only PSI resides and others where only PSII is present. Similarly, the protein content of the thylakoid tubules that traverse the pyrenoid differs from the other regions of the thylakoid membrane across algal lineages [55, 80, 88, 117, 118]. Some protein variation could be explained by specific targeting of RBM containing transmembrane proteins to the pyrenoid tubules [101], but distribution variation in many proteins that lack RBMs, such as PSI and PSII subunits, is unknown.

In addition, the biogenesis of the pyrenoid tubules and minitubules remains completely unresolved. In many algal species, the thylakoid membrane drastically changes as it enters the pyrenoid matrix. In *Chlamydomonas*, the stacked membrane layers of the thylakoid membrane merge into one cylindrical tubule per stack that engulfs smaller minitubules as they approach the pyrenoid (Figure 3 and 4; [51]). In the centre of the pyrenoid these tubules merge to form an interconnected network. The factors that transform the thylakoid membrane from multiple stacked membrane layers into highly curved tubules remain unknown. Recently, it has been shown that LLPS on the surface of liposomes can lead to the formation of invaginations in the liposomes that can develop into lipid tubules [119]. However, in pyrenoid-less *Chlamydomonas* strains (where the Rubisco SSU is exchanged for the SSU of higher plants, which do not bind EPYC1) the pyrenoid tubule network in the centre of the chloroplast seems largely unaffected in TEM images. This suggests that LLPS on the membrane surface is not responsible for the formation of the pyrenoid tubules and the pyrenoid tubules might form independently from pyrenoid matrix assembly [120]. Yet, we lack high-resolution 3D images of the tubule network in these strains to ensure that the network is not altered in any way due to the absence of the pyrenoid matrix. Even though it seems plausible that the pyrenoid matrix is involved in formation and shaping of the pyrenoid tubule network it seems likely that membrane fusion/fission and curvature inducing proteins, which are also involved in thylakoid biogenesis [121], are part of these processes.

PYRENOID DYNAMICS

The pyrenoid of *Chlamydomonas* displays many of the characteristics of LLPS bodies, with both *in vivo* [36] and *in vitro* [44] studies providing multiple levels of support. This section will outline this supporting evidence and highlight our current state of knowledge and open

questions related to pyrenoid dynamics including division, regulation of pyrenoid LLPS, and pyrenoid nucleation. Whereas most of our experimental data comes from *Chlamydomonas*, decades of observations across diverse algae provide translational insights into pyrenoid dynamics.

Evidence for Pyrenoid LLPS

Thanks to the work of Freeman Rosenzweig et al. [36], some of the classical hallmarks of liquid droplets initially described by Brangwynne et al. [24], including fusion, dissolution, *de novo* formation and internal rearrangement, have all been observed over second timescales in the *Chlamydomonas* pyrenoid. In this study, *in situ* cryo-ET also revealed that Rubisco molecules in the pyrenoid exhibit short-range distribution patterns, characteristic of liquid-like order. The additional *in vivo* observations that pyrenoids adopt a largely spherical morphology that can be reversibly deformed and appears to be wetted to the surrounding starch sheath provide additional fundamental support for the LLPS nature of the pyrenoid [122]. These *in vivo* observations were bolstered by the work of Wunder et al. [44], who showed that a minimal *in vitro* reconstituted pyrenoid matrix (Rubisco and EPYC1) possessed many similarities to its *in vivo* counterpart over complementary timescales. Here it was demonstrated that functional Rubisco could be demixed by the linker EPYC1 under physiologically relevant conditions and concentrations in a valency-dependent manner. Further, fluorescence recovery after photobleaching (FRAP) analysis indicated the reconstituted droplets rearrange over similar timescales to those observed *in vivo* [36], and thus provide a suitable proxy for the LLPS of the pyrenoid.

Pyrenoid inheritance

During mitotic division of vegetative cells, approximately two thirds of *Chlamydomonas* daughter cells inherit pyrenoids via fission, with the remaining daughter cells either asymmetrically inheriting the whole mother-cell pyrenoid (~20%), forming a *de novo* pyrenoid from dilute stromal Rubisco (~6%) or failing to inherit a pyrenoid (~8%) [36]. Fission [123] and *de novo* [124-126] pyrenoid inheritance are classically described in green algae, but have also been described in hornworts and non-green lineages (fission: [127-130]; *de novo* assembly: [131-136]), where both mechanisms appear equally prevalent. Besides *Chlamydomonas*, multiple concurrent pyrenoid inheritance mechanisms have only been reported in *Arachnochrysis demoulinii* sp. nov. (stramenopila; [39]) and *Chlorogonium elongatum* (chlorophyta; [137]). It is unlikely this is unique to these species and is instead likely reported due to more intensive characterizations. Anecdotally, *de novo* pyrenoid formation following division appears to be reported more commonly in species where vegetative cells possess multiple distinct pyrenoids. This observation appears to extend across lineages, but exceptions do exist in some chlorophyta [138, 139] and the definition of ‘multiple pyrenoids’ becomes unclear, especially in multicellular hornworts [140]. Pyrenoid fission is typically induced by plastid constriction, or less commonly, starch sheath invagination [123]. With pyrenoid fission driven by plastid constriction being documented across lineages: green algae (chlorophyta) [141], haptophytes (haptophyta) [142], hornworts (bryophyta) [130, 143], diatoms (stramenopila) [144, 145], brown algae (stramenopila) [131, 146], red algae (rhodophyta) [129, 147] and dinoflagellates (alveolata) [148].

In *Chlamydomonas,* fission occurs over an ~7 minute window at the end of the chloroplast division (~30-80 minutes), suggestive of a mechanical interference by the plastid cleavage furrow [36], consistent with the observations of Goodenough [141]. The cleavage furrow advances across a symmetry axis that is important for maintaining the polarity of the

cell following cytokinesis [149, 150]. Chloroplast division in plants has been shown to be synonymous with the widely conserved contraction of a stromal ring-like FtsZ structure [151, 152] positioned by MIN proteins [153], presumably inherited from cyanobacterial ancestors [154]. Homologous systems are present in algae [139, 155-158], but there is little clarity on their roles in plastid division mainly due to lack of conserved transcriptional patterning [157, 159-161], and formation of multiple conglomerate FtsZ rings [162, 163]. F-actin has also been implicated in facilitating furrow progression at the chloroplast to aid subsequent chloroplast division in *Chlamydomonas* [164] and two species of red algae [165, 166], where it could provide a structural signal [167, 168], but this role is hypothetical. Clearly more work is required to definitively determine the forces driving plastid division in algae, and the implications this has on cleavage furrow progression and pyrenoid fission. Whether furrow-induced pyrenoid fission is underpinned by molecular interactions or is the result of a purely mechanical interference also remains to be seen. The dynamic distribution of pyrenoid ultrastructural features (starch and thylakoid material) throughout division is unassessed in *Chlamydomonas*, and has been sparsely reported in other pyrenoid-containing species. In *Leptosiropsis torulosa* (chlorophyta) however, the starch is reported to divide between daughter pyrenoids from the mother [169]. Given the apparent importance of starch in form and function of the pyrenoid, it is likely that coordinated distribution of starch (when present) through divisions is equally important [42, 91]. In *Porphyridium cruentum* (rhodophyta) the traversing thylakoid material is divided between the daughter cells [127]. Likewise, Lokhorst and Star [170] report even distribution of both starch and thylakoid structures through pyrenoid fission in *Ulothrix* (chlorophyta). The canonical positioning of the pyrenoid at the tubule network suggests that symmetrical segregation of this network between daughter cells will be equally important for correct pyrenoid retention and reformation through cell division [51].

Intriguingly, in *Chlamydomonas* towards the end of chloroplast division and prior to pyrenoid division under constant light, a significant portion (~35-50%) of the Rubisco/EPYC1 disperses from the pyrenoid into the surrounding stroma [36]. It is expected that this dispersion will reduce pyrenoid viscosity and surface tension and accordingly reduce the mechanical force required for pyrenoid fission by the centrally positioned cleavage furrow, in line with physical theory [171]. Freeman Rosenzweig et al. [36] also note, in cell divisions where the pyrenoid does not appear to be bisected during cytokinesis, pyrenoid fission is not observed. This might suggest a primarily mechanical driving force for fission, but it is possible that incorrect segregation of unresolved ultrastructural features also play a role. The interference of the cleavage furrow on pyrenoid ultrastructure is not well studied, but the classical observations of the green algae *Tetracystis isobilateralis* by Brown et al. [172] suggest a role for pyrenoid traversing chloroplast thylakoids in division. A thylakoid membrane-oriented pyrenoid division mechanism is plausible given the recent reports of endoplasmic reticulum membrane contact with liquid droplet P-bodies in directing their fission location and propensity [108]. Collectively, the above observations highlight the importance of the canonical positioning of the pyrenoid and cleavage furrow during cell division to facilitate pyrenoid inheritance through fission. When either of these positional requirements are awry, pyrenoid fission does not occur, and one of the daughter cells inherits the mother pyrenoid, leaving its sister pyrenoid-less. In the pyrenoid-less daughter cell, ~50% form pyrenoids *de novo* from coalescence or apparent Ostwald ripening of multiple incipient pyrenoid puncta in the chloroplast stroma [36], similar to descriptions in hornworts [173]. The sites of *de novo* formation are not well described, but the observations of Bisalputra and Weier [174] suggest an interplay with thylakoids in other species. These observations suggest an important role for thylakoid membranes in pyrenoid division and *de novo* assembly.

In addition to facilitating pyrenoid fission, the relocation of Rubisco and EPYC1 to the chloroplast stroma may have evolved as a safeguard to provide a basal level of Rubisco to the daughter cells for rapid *de novo* pyrenoid formation in the absence of fission [36], similar to P granule relocation by re-condensation [24]. This has been proposed to facilitate Rubisco inheritance through division in the multiple pyrenoid-containing cells of hornworts [140], and is a plausible explanation for the observation of common *de novo* formation in other multiple pyrenoid-containing species, where coordination of furrow-induced fission is more difficult. The lack of high-resolution studies outside of the green lineage makes translation of these observations difficult, and it is possible diverse pyrenoid-containing species operate distinct pyrenoid distribution mechanisms. Even in *Chlamydomonas* there are multiple open questions (Figure 5), such as: What happens to pyrenoid ultrastructural features throughout division? What determines plastid fission and cleavage furrow positioning? What determines the site of *de novo* pyrenoid assembly? Is the basis for fission solely mechanical?

Regulation of pyrenoid dynamics

Although the dynamic, liquid-like properties of the *Chlamydomonas* pyrenoid have been well characterized, very little is known about their regulation. In this section, we discuss the possible regulatory mechanisms at play (summarised in Figure 5B), relating existing pyrenoid data and the wealth of control mechanisms demonstrated in other biomolecular condensates (see Dignon et al. [30] and Owen and Shewmaker [35] for recent reviews). As discussed previously, the pyrenoid exhibits several apparent phase transition events that occur over different timescales, and we discuss their potential control mechanisms accordingly.

Pyrenoid dynamics over short timescales

The rapid nature of pyrenoid dynamics throughout cell division (dissolution and *de novo* formation) has generated considerable interest in the role of post-translational modifications (PTMs) through these events [36], given widespread reports of their role in regulating analogous condensates [35, 175]. Given that intrinsically disordered proteins are frequently modified post-translationally due to their conformational accessibility [176], it appears probable that PTM of EPYC1 will play a role in pyrenoid dynamics. Although PTMs of globular domains are more sparsely reported in coacervation control, with reports limited to ribonucleoprotein granule component TDP-43 [177], here we also discuss the possibility of PTM of Rubisco to effectively modulate valency and, thereby, control the size and physical properties of the aggregate. These considerations are made under the assumption that matrix components (Rubisco/EPYC1) are readily modified both within the dilute stromal and condensed matrix states, as has been described in other 'active' condensates [178, 179].

Phosphorylation: Given that many biomolecular condensates incorporate phosphatases and kinases that regulate the phosphorylation state and essential interactions of component molecules that ultimately determine phase dynamics [29], there is considerable interest in exploring the phospho-states of pyrenoid matrix components. The rapidly achieved, highly phosphorylated state of EPYC1 in light under low CO_2 (where nearly all Rubisco is condensed in the pyrenoid) conditions [180, 181] has led to suggestions that the phosphorylation state of EPYC1 may control phase separation, by affecting Rubisco binding valency [80, 182]. Turkina et al. [180] showed that phosphorylation of EPYC1 in response to CO_2 limitations occurs at serine and threonine residues within the flexible regions between the Rubisco interaction helices [95, 97, 183]. Alongside tyrosine, phosphorylation of serine/threonine residues has been shown to both enhance and hinder phase separation dynamics in other systems, through

recruitment and interaction screening effects respectively [35]. Here we discuss the role of phosphorylation-enhanced valency, given the correlation with pyrenoid formation, but acknowledge the absence of definitive evidence.

Interaction data supports EPYC1 association with two 14-3-3 phospho-binding proteins, FTT1 and FTT2 [80]. 14-3-3 proteins are highly conserved proteins that are implicated in a multitude of biological phosphorylation regulated processes across the eukaryotic tree of life [184, 185], with diverse and often contradictory functions, including protein binding occlusion, induced conformational change and interaction scaffolding [185]. 14-3-3 binding potentially occurs at one of EPYC1's phosphorylated serine residues that resides within an almost complete 14-3-3 binding motif ([R].[S].[X].[pS].[X].[P] [186]), that is repeated 3 times within the EPYC1 sequence [186]. Given the phosphorylation state of EPYC1, 14-3-3 proteins would therefore be expected to be bound in low CO_2 conditions, and may explain low CO_2 dependent pyrenoid formation potentially through interaction scaffolding by increased linker protein valency or self-association, as observed in other complex coacervates [187, 188].

Besides a potential 14-3-3 binding role, our understanding of EPYC1 phosphorylation effects is limited. No interacting pyrenoid kinases or phosphatases were highlighted from interactome studies [80], and our understanding of the effects of phosphorylation on the EPYC1-Rubisco interaction are lacking. The presence of the phosphorylation sites outside of the interacting regions of EPYC1 might suggest that there is no large impact on the interaction with Rubisco. Equally, modifications within flexible regions have been shown to enhance phase separation in other condensates [32, 187], but our understanding here is sparse. A detailed study of EPYC1 phosphorylation, that highlights potential kinases/phosphatases and assesses the Rubisco interaction would provide insight into the correlated process of pyrenoid formation and EPYC1 phosphorylation.

Methylation: Residue-specific methylation has also been shown to have wide-reaching effects on droplet formation in other systems, primarily through arginine-associated modifications [35]. Two candidate methyltransferases have been implicated in the CCM, and we discuss these separately below. Although these methyltransferases are predicted to act on lysine, its similarity to arginine and the apparent monomethylation of lysine at three sites in EPYC1 under low CO_2 conditions warrant its consideration in pyrenoid dynamics [80]. Mutants of the first methyltransferase, CIA6, fail to form a canonical pyrenoid and exhibit growth phenotypes similar to the mutant of the linker protein, EPYC1 (failed pyrenoid assembly and no CCM) [51, 189]. This phenotype presumably indicates reduced EPYC1 accumulation, or a reduced interaction with Rubisco, given that Rubisco accumulates to the same level in this strain and that CIA6 appears not to methylate Rubisco *in vitro*. Ma et al. [189] also demonstrate reduced levels of CCM components in the *cia6* mutant, but do not assess EPYC1 accumulation. Establishing the transcript and protein levels of EPYC1 in this mutant would facilitate disentangling the two possibilities for failed pyrenoid formation here. Interestingly, EPYC1's methylation sites lie within the 'SKKAV' motif that Wunder et al. [44] hypothesised could drive EPYC1's interaction with negative patches of Rubisco. Although methylation does not affect the charge of residues and would therefore be unlikely to disrupt these non-specific charge interactions, methylation at these sites would presumably preclude residue-specific cation-π interactions, that could otherwise enhance valency.

The second putative methyltransferase, SMM7, has been localized to the pyrenoid matrix [80], and is significantly upregulated in low CO_2 conditions, unlike CIA6 [190, 191], but no phenotypic data is available. SMM7 bears homology to calmodulin dependent METTL21

proteins that methylate molecular chaperones to regulate their activity [192]. However, there is currently no evidence to support this function for SMM7. Phenotypic analysis of SMM7 mutants with respect to EPYC1/Rubisco accumulation and methylation profiles should be completed to further probe the role of methylation in pyrenoid assembly. It is equally possible Rubisco methylation could contribute to perturbations in pyrenoid assembly, but methylation profiles of Rubisco are not currently available across phase transitions.

Other post-translational modifications: Other PTMs, including lysine acetylation, arginine citrullination and poly(ADP-ribosylation) have been implicated in phase separation dynamics [35], but these are unexplored in *Chlamydomonas*. The observation that recombinant EPYC1 can phase separate *in vitro*, presumably in the absence of physiological PTMs [44], may imply that the above potential modifications are not major determinants in coacervate formation, but may play a role in the disassembly process that occurs during cell division and acclimation to high CO_2 environments.

Pyrenoid dynamics over longer timescales

In contrast to the rapid pyrenoid phase transitions that occur prior to, and following cell division, those that occur in response to CO_2 [193] and light [194] changes potentially occur over significantly longer timescales (several hours). Although it is likely that PTMs play a role in the regulation of these transitions, here we discuss the influence of global changes in cellular physiology that could explain the slower response and have been implicated in the transitions of other systems. These include pH [195, 196], temperature [197, 198], salt concentrations [197] and osmotic pressure [199].

pH: The pH of the stroma markedly increases under light-dependent photosynthetic conditions in higher plants [96], cyanobacteria [12] and algae [200], due to the pumping of protons from the stroma into the thylakoid lumen. Under extended dark conditions the pyrenoid of *Chlamydomonas* dissolves and Rubisco transiently relocalizes to the stroma [194]. The correlation of photosynthetic stromal pH change and pyrenoid presence across light conditions warrants interest in the effects of these changes on pyrenoid formation and function. In cyanobacteria and algae, the photosynthetic pH rise increases the prevalence of HCO_3^- over CO_2 in the stroma, and likely enhances CCM efficiency using specialized HCO_3^- transporters/channels that increase flux to Rubisco condensates [201]. Given the non-membrane bound nature of the pyrenoid, it is expected that stromal pH increases (from ~7 in the dark to ~8.5 in the light) will be mirrored in the pyrenoid matrix, with only slight variations due to localized diffusive fluxes [96]. pH changes of this magnitude (~1.5 pH units) have been shown to influence charge interactions by protonation/deprotonation of clustered charged residues in the “pH sensor” domain of Sup35, where upshifted pK_a values are thought to contribute a pH-sensitive function at physiological pH [196]. A similar process may promote Pub1-directed pH-dependent stress granule assembly [202].

The Rubisco-interacting helices and ‘SKKAV’ motif represent the main charge clustering in the EPYC1 sequence and could contribute a similar function in *Chlamydomonas*. Alternatively regions of negative charge on the surface of the Rubisco SSU highlighted by Wunder et al. [183] could behave similarly, especially given the more notable shift in pK_a of residues in local charge regions of globular proteins [203]. However, although electrostatic screening effects have been probed *in vitro* [44], the pH-sensitivity of EPYC1-Rubisco demixing remains uncharacterized.

Concentration of pyrenoid components: The concentration of proteins and their associated valencies clearly defines condensate assembly and composition [22]. Many primary pyrenoid matrix components are differentially abundant across the light-dark and low-high CO_2 transitions, in correlation with the dissolution/relocalization of the pyrenoid and its components [51, 194]. Certainly, the timescale for protein expression could provide a time-appropriate explanation for the apparent slower pyrenoid dynamics observed across these transition periods.

Both the Rubisco large and small subunits are consistently abundant throughout the light-dark and low-high CO_2 transitions which would negate a concentration-dependent role for them [194]. Contrastingly, EPYC1 displays differential abundance at both the transcript and protein level across both the light-dark and low-high CO_2 transitions [51, 180, 190]. It is possible these abundance changes could drive phase transitions observed *in vivo*, consistent with linker concentration-dependent demixing effects observed in analogous systems [187]. Although protein abundance has been charted well across these transitions, the distinct mechanisms of transcriptional control, cytoplasmic shuttling, chloroplast import and degradation of EPYC1 are unexplored (Figure 5). These processes are undoubtedly entangled with the aforementioned molecular modifications, but their interdependence and implications remain unelucidated.

Temperature: Temperature is not likely to markedly affect pyrenoid formation and division dynamics, given the low CO_2, pyrenoid-dependent growth of *Chlamydomonas* across wide temperature ranges [204]. In line with this observation Wunder et al. [44] also reported no significant shift in phase diagram across a range of physiologically relevant temperatures (0-40 °C) for *in vitro* Rubisco-EPYC1 demixing. At a superficial level, the pyrenoids of cold-water species are largely ultrastructurally similar to those of temperate species (for examples see references [205-209]), indicating no major change in pyrenoid assembly.

It will be interesting to consider the characteristics of pyrenoids that form in cold-adapted species such as *Chlamydomonas* sp. UWO241, where photosynthesis is adapted to exhibit comparable rates to species grown at ambient conditions [210, 211]. Whether pyrenoids in cold-adapted species exhibit the same dynamic properties observed in temperate pyrenoid species is unknown. It has been reported that the linker protein EPYC1 is downregulated during low CO_2 cold adaptation in *Chlamydomonas* [212], but whether this has functional implications is unknown. In *Anthoceros* hornworts, pyrenoid shape has been reported to change in response to cold-adaptation, from spindle-shaped to round [135], perhaps suggesting an active process underpins maintenance of the spindle shape. These observations likely suggest that temperature does not play a unique role in pyrenoid dynamics, but study of matrix properties in cold-adapted species would nevertheless provide valuable insight into the role of macroscopic properties (surface tension, viscosity) on pyrenoid function.

ATP and Ionic strength: Given the largely active state of many condensates in maintaining their liquid-like properties through enzymatic processes [179], ATP concentration has been proposed to play a role in biological phase separation events [30], given its role as a biological hydrotrope [213]. As discussed previously, the ultrastructure of the pyrenoid has been proposed to allow the exchange of ATP with the chloroplast stroma, facilitating activity of the highly active canonical AAA+ ATPase chaperone, Rubisco activase (RCA) [214], amongst other enzymes [79]. The presence of active PSI, and its associated cyclic electron transport processes inside the pyrenoid could provide an alternative source of ATP for these processes [80, 88]. RCA remodels Rubisco in the pyrenoid [215], and its ATP-consumptive activity is

related to the photosynthetic state of the cell [216]. In *Chlamydomonas*, RCA is located in the pyrenoid [80, 217], where it has similar mobility to RBCS1, presumably to enable its dynamic role [36]. It is possible that this presumably large change in flux of ATP when the photosynthetic state of the cell changes plays a role in phase dynamics. However, pyrenoid phase dynamics in response to flux changes in ATP and other key metabolites (RuBP, 3PGA, HCO_3^-) are largely unassessed in *Chlamydomonas*.

Similar to ATP-dependent dynamics, ionic strength has been implicated in disassembly of analogous condensates, where electrostatic interactions dominate [197]. Notably, the *in vitro* demixing of the N-terminal domain of α-carboxysome linker CsoS2 with Rubisco requires low salt concentration [43], analogous to the salt-dependent demixing of EPYC1 and Rubisco. In addition to the proposed pH-dependent effects on electrostatic interactions in the pyrenoid, spatiotemporal Ca^{2+} fluxes provide an additional layer of charge effects. CAS1, a Ca^{2+}-sensing protein, re-localizes to the pyrenoid upon CCM induction, possibly facilitating a CO_2 response that facilitates assembly of key CCM components [218, 219]. It was also determined that pyrenoid Ca^{2+} concentration is markedly increased in low CO_2 conditions [218]. The increased Ca^{2+} concentration would presumably screen electrostatic interactions and subsequently disfavour phase separation of the pyrenoid. Whether these charge fluxes definitively affect the putative electrostatic interaction between Rubisco and EPYC1 in the pyrenoid matrix is undetermined, but electrostatic dependence of demixing is readily observed [44]. *In vivo* quantification of ionic strength in the pyrenoid, using established methods [220], could provide useful insight here.

Pyrenoid size

Pyrenoid size increases following division due to Rubisco recondensation and likely increases due to CCM-induced relocalization [36, 194]. Across mature *Chlamydomonas* cells pyrenoid size is largely consistent under the same growth conditions and appears to scale with cell size during growth [42, 51, 221]. Rubisco-EPYC1 droplets are not size-limited *in vitro*, suggesting that pyrenoid size is component limited *in vivo* [44], as observed in other biomolecular condensates [25]. Alternatively, physical restrictions determined by other ultrastructural features (starch/thylakoids) could limit droplet size. In a multiple pyrenoid-containing mutant of the starch-associated Rubisco-binding protein SAGA1, the total pyrenoid matrix area is decreased (indicating that pyrenoid volume is also decreased) despite Rubisco levels remaining unaffected [42]. Thus, indicating that disrupted interactions between the pyrenoid matrix and the starch has an effect on pyrenoid number and matrix area, however it has to be noted that the exact functional role of SAGA1 is still unclear and similar multiple pyrenoid phenotypes are also seen in EPYC1 and CIA6 mutants. At a biophysical level, the implications of pyrenoid size relating to macroscopic properties, such as surface tension and viscosity are unexplored.

Pyrenoid dissolution

High resolution spatiotemporal data is lacking for *Chlamydomonas* pyrenoid dissolution across the slower low CO_2 to high CO_2 and light to dark transitions, though partial dissolution prior to cell division is characterized over an ~20 minute window [36]. In the closely related ulvophyceae, *Ulva linza* and *Ulva intestinalis* (chlorophyta), dark-induced dissolution appears to occur over many hours [222], with a similar result observed in *Scenedesmus acuminatus* (chlorophyta) [223]. No data is available for high CO_2 transitions.

As aforementioned, it is likely the rapid phase transition observed prior to division is regulated at the post-translational level and suggests fine control over phase dynamics within

the cell. Following pyrenoid dispersing phase transitions, a portion of the matrix is retained at the canonical pyrenoid position (centred on the thylakoid network intersection) (Figure 5B) [120, 194]. The retained portion contains both Rubisco and EPYC1 [36]. Interestingly, a similar phenomenon is observed in the 'pyrenoid-less' *epyc1* mutant [51], where a portion of the Rubisco is maintained at the stellate thylakoid network. QFDEEM data indicate this aggregation has a lower packing density than the pyrenoid, presumably due to the absence of EPYC1 driven Rubisco packaging [51]. The presence of RBMs found in several pyrenoid components that localize to distinct sub-pyrenoid regions [101] may explain this residual Rubisco matrix at the canonical pyrenoid position in the *epyc1* mutant.

Crucially, the fate of EPYC1 during dissolution is not determined, with possibilities including degradation, dissolution into the stroma as monomers (or homo-multimeric complexes) or dissolution into the stroma as small EPYC1-Rubisco heteromeric assemblies. Given that Rubisco is consistently abundant throughout transitions, the level of EPYC1 protein abundance is likely pivotal in determining pyrenoid reformation following dissolution. EPYC1 degradation rates over pyrenoid division and CCM state changes are yet to be characterized, but could hold vital clues for the dissolution and re-condensation mechanisms of the pyrenoid (Figure 5A).

Pyrenoid nucleation

Nucleation of phase separated condensates is crucial to their dynamic functions and cellular positioning, and requires surmounting a kinetic barrier [19]. This process can occur homogeneously through random fluctuations at non-defined locations, or heterogeneously at pre-existing sites, where pre-assembly seeds droplet formation [25]. *De novo* formation of pyrenoids in the stroma has been documented widely. Observations in *Chlamydomonas* show that multiple proto-pyrenoid puncta can form *de novo* in the stroma of daughter cells. One of these puncta appears to form at the canonical position of the pyrenoid in the chloroplast, and over time grows to become the main Rubisco aggregation in the stroma, whilst the other puncta diminish [36]. Very little is known about this process, but recent evidence provides some insight.

Nucleation at the canonical pyrenoid position is perhaps explained by enhanced Rubisco accumulation. In parallel to RBMP1/2 potentially acting as tethers of the pyrenoid matrix to tubules, they could also play a pivotal role in the initial recruitment of Rubisco to the pyrenoid tubules to drive pyrenoid assembly [101]. As described above, SAGA1/2 are suggested to play a role in pyrenoid assembly through starch adherence to the pyrenoid matrix [101], however the role of these starch-associated proteins should not be overlooked when interrogating pyrenoid nucleation. SAGA1/2 belong to a suite of coiled-coil containing proteins associated with the pyrenoid, many of which appear to associate with starch [42, 80]. The association of coiled-coil domains has been shown to provide structural scaffolds for droplet formation and positioning in several membraneless organelles [29], and thus coiled-coil containing proteins could play a role in pyrenoid nucleation.

Subsequent growth of the canonically positioned matrix is unexplored, but has multiple potential explanations based on descriptions of other biological condensates. If the droplet nucleated at the canonical position has a larger droplet size, due to pre-seeding or concentration-dependent effects, Ostwald ripening would preferentially drive the growth of this droplet (Figure 1) [224]. Similarly, growth could be driven by elastic ripening, in which the transport of solute down a stiffness gradient results in the preferential growth of droplets at areas of low stiffness, on a faster timescale than Ostwald ripening [26, 225] (Figure 5B). Mechanical heterogeneity within the *Chlamydomonas* chloroplast has not been characterised,

but it is possible the absence of thylakoid stacks at the canonical position contributes reduced network stiffness and facilitates a stiffness gradient [226].

De novo formation of multiple proto-pyrenoid puncta in the stroma of daughter cells suggests nucleation also occurs separate to the canonical pyrenoid position. It is possible that fluctuations in local concentrations of EPYC1 and Rubisco could provide a basis for nucleation, independent of structural features that contribute seeding effects. Additionally, given the rapid timescale for nucleation and re-condensation following division (<1 hour), it is likely the same PTM control mechanisms important for dissolution are also poignant here. Similarly, light-induced re-condensation occurs during an ~4 hour window [194], with low CO_2-induced reformation occurring over similarly longer timescales [193], suggesting alternate mechanisms for controlled nucleation in these instances.

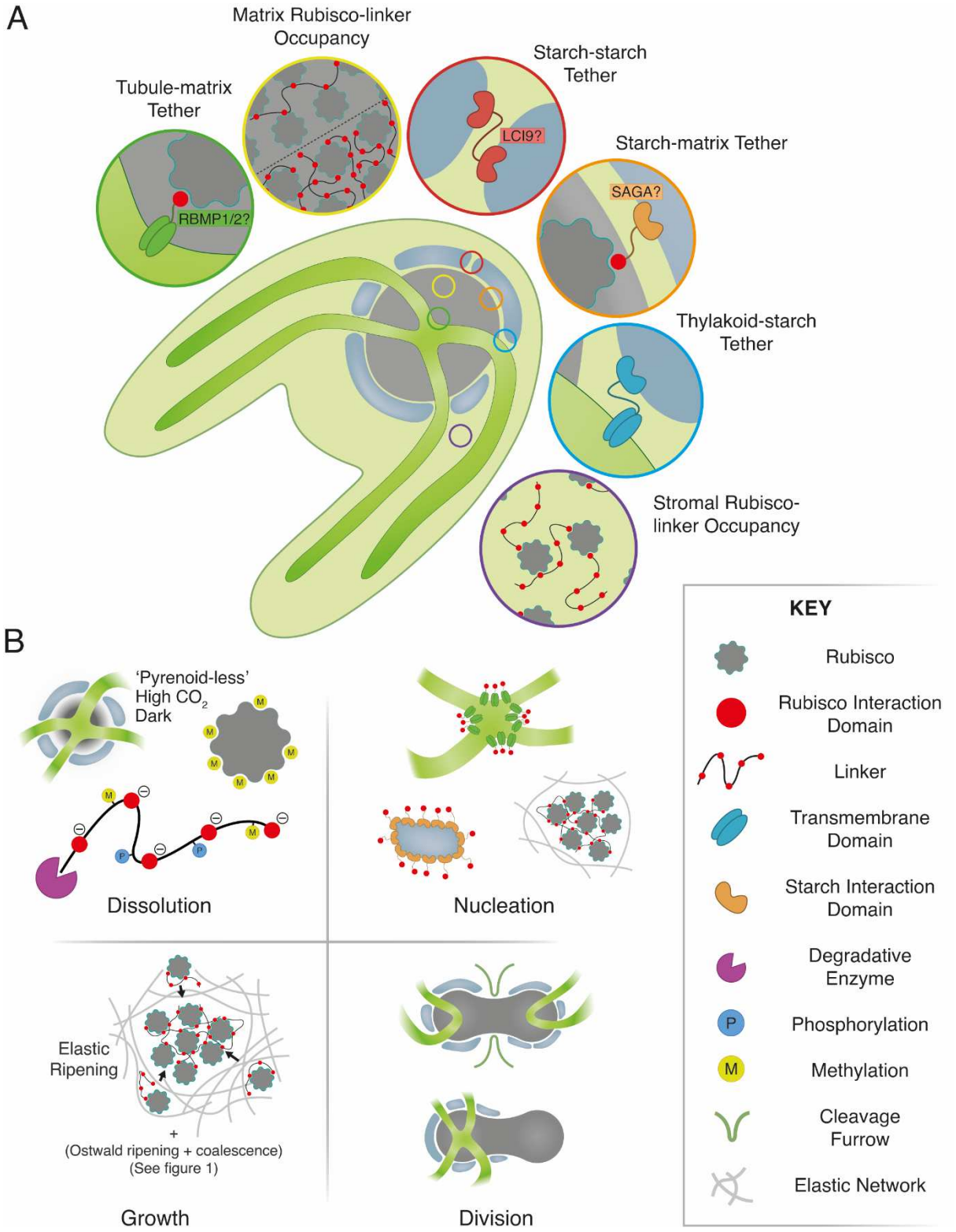

Figure 5. Key unanswered questions in the *Chlamydomonas* pyrenoid. A) Molecular basis for pyrenoid localization at key ultrastructural features (clockwise from top left). A predicted pyrenoid tubule-enriched Rubisco-binding protein that could contribute to canonical positioning and localization of the pyrenoid matrix, as in B, perhaps contributed by RBMP1/2. The unknown occupancy of the Rubisco-linker interaction that underpins LLPS of the matrix, where the dashed line demarcates a low Rubisco, high linker occupancy and a high Rubisco, low linker occupancy scenario. A putative protein interaction that spans the inter-starch gaps in the sheath to tether

adjacent plates, possibly fulfilled by LCI9, as highlighted in Mackinder et al, [80]. A starch-associated Rubisco-interacting protein that tethers the starch sheath to the matrix, possibly underpinning an alternative starch-centric nucleation model, as in B, perhaps performed by SAGA1/2 [42] among others. A putative thylakoid-associated, starch-binding protein that could explain the canonical positioning of the starch plates in pyrenoid-less strains. The uncharacterized occupancy and oligomeric state of the Rubisco-linker interaction in the dilute stromal phase. **B)** Potential control mechanisms underpinning the dynamics of the pyrenoid. Dissolution, clockwise from top left. The dissolved state of the pyrenoid, showing canonical positioning of the starch plates and retention of a portion of the matrix at the tubule intersection, possibly forming an interdependent assembly point. A methylated state of Rubisco that could disrupt linker interactions and contribute to dissolution. Potential linker perturbations that could contribute to phase transitions, including PTMs (phosphorylation and methylation) as well as degradation (concentration effect) and charge perturbation (pH and ion concentration). Nucleation, from top left. Tubule-enriched matrix tethers, that could nucleate a canonically positioned pyrenoid, consistent with A. Spontaneous nucleation at a region of low elastic density in the stroma. Starch-centric nucleation, seeded by starch-matrix tethers, consistent with A. Growth, multiple explanations for pyrenoid growth following *de novo* formation. Division, possibilities for ultrastructural distribution through cleavage furrow-induced pyrenoid fission.

DOES LLPS UNDERPIN PYRENOID ASSEMBLY ACROSS LINEAGES?

Pyrenoids in all lineages consist of an electron-dense matrix that is believed to be a Rubisco condensate. This assumption is based on observations across pyrenoid containing lineages that the pyrenoid matrix contains most of the cell's Rubisco [55, 70, 71, 88, 133, 140, 217, 227-232]. To date there is only conclusive evidence in *Chlamydomonas* that the pyrenoid is a LLPS organelle [36, 44], however there are several lines of evidence that suggest that pyrenoids are LLPS across diverse lineages. Pyrenoids normally have spherical/elliptical shapes, which is typical for organelles formed by LLPS and not bound by membranes, given their surface tension effects. As outlined above, the observation of pyrenoid division via fission and examples of *de novo* assembly and apparent Ostwald ripening also supports the idea that LLPS is a general property of all pyrenoids. In addition, dissolution of the pyrenoid and dynamic Rubisco relocalization has been reported across diverse algae including the dinoflagellate *Gonyaulax* [233] and the green alga *Dunaliella tertiolecta* [234] and *Euglena gracilis* [133].

Along with observational evidence, bioinformatic analysis revealed the occurrence of proteins in a broad range of algae that show similarities to the *Chlamydomonas* Rubisco linker protein EPYC1 [51]. These proteins have a similar repeat number, length, isoelectric point and disorder profile to EPYC1 indicating a putative function as linker proteins. All in all, the observed spherical shape of the pyrenoid, the observation of pyrenoid fission and identification of proposed Rubisco linker proteins, suggests that pyrenoids are formed by LLPS across algal lineages. However, essential experimental evidence to support pyrenoid LLPS in diverse algae is missing.

PYRENOID EVOLUTION

Even though pyrenoids occur in all algal lineages and in hornworts, not all algae or hornwort species contain pyrenoids. Pyrenoid-less algae (e.g. the extremophile rhodophyte class *Cyanidiophyceae*, members of the chlorophyte genera *Bathycoccus* and *Chloromonas*, the TSAR class chrysophyte (golden algae), and most species of the eustigmatophyte genus *Nannochloropsis*) and hornworts that lack pyrenoids are spotted across the phylogenetic tree,

suggesting that pyrenoids were lost and gained multiple times during evolution [50, 235, 236], possibly with hundreds of evolutionary origins [15]. The exact distribution of pyrenoids is unknown since the anatomy of many algae has never been investigated thoroughly. Moreover, the occurrence of a pyrenoid in different algal species could depend on factors such as CO_2 abundance, light and life-cycle stage. Thus, the apparent absence of pyrenoids in some species might be attributed to the metabolic state of the imaged cells, life-cycle stage or even missed due to insufficient imaging.

The evolutionary history of the pyrenoid is complex and presently poorly understood. Our best understanding of pyrenoid evolution comes from hornworts where pyrenoids have evolved at least 5-6 times independently and have also been lost at least 5-6 times [50]. The first hornwort pyrenoids appeared ~100 million years ago, a time that coincided with a drastic decline of atmospheric CO_2 levels. However, other younger pyrenoid-containing clades originated during periods with higher atmospheric CO_2 levels and pyrenoids were apparently lost in hornwort clades during periods with relatively low atmospheric CO_2 levels [50]. Taken together, these findings suggest that pyrenoids in hornworts did not evolve solely as a response to atmospheric CO_2 levels but must also offer further evolutionary advantages. Hornworts are typically found in terrestrial habitats growing on soil banks or epiphytic on trees and leaves but can also be semiaquatic growing partially submerged or undergoing temporal submersion in freshwater habitats [237]. In algae, the evolution of pyrenoids and a biophysical CCM is widely considered as an adaptation to their aquatic lifestyles, where HCO_3^- is more abundant than CO_2 and the CO_2 diffusion to Rubisco is limited [238]. However, this adaption to aquatic environments is not clear in hornworts, with some semiaquatic hornwort species lacking pyrenoids, whereas several terrestrial hornwort species contain pyrenoids [237].

It has been proposed that the lack of pyrenoids in all other land plants indicates that the last common ancestor of all hornworts had no pyrenoid and that pyrenoids in hornworts evolved independently of ancestral algal pyrenoids [50]. However, recent genomic data is offering some new insights into pyrenoid evolution [239]. Some pyrenoid localized core green algal CCM components, like LCIB and CAH3, appear to have homologs in hornworts (but not land plants), while others, like EPYC1 or RBMP1/2, have no homologs (although sequence divergence may be accelerated for intrinsically disordered proteins). This suggests that the common ancestor of green algae and hornworts (and hence land plants) may have had a biophysical CCM. With biophysical CCM loss at both a genetic and functional level occurring in land plants but retained in hornworts (at least at a genetic level) with the then subsequent loss or replacement of individual components during pyrenoid and CCM loss and re-acquisition during hornwort evolution. The identification of analogous pyrenoid components across lineages will likely shed some light on pyrenoid evolution.

Pyrenoid structural diversity across different algal lineages

Pyrenoid structure varies greatly between different algal and hornwort species (Figure 6). Common to all pyrenoids is that they consist of a dense Rubisco matrix, which is probably formed through LLPS (see discussion above). Variation in matrix staining across species suggests differences in matrix protein concentration but could also be due to fixation artefacts and differences in fixation protocols. Of note, found within the matrix of some hornwort and all *Trebouxia* (chlorophyta) lichen symbionts are lipid-rich globules called pyrenoglobuli [140, 240]. Whereas most species have only one pyrenoid per chloroplast, some species have two or more [23, 170, 241, 242], sometimes even ultrastructurally distinct pyrenoids [243]. In the chlorophyte *Spirogyra*, each chloroplast has multiple evenly-sized pyrenoids [23, 242], suggesting that Rubisco condensation is controlled by an unknown mechanism, which

prevents Ostwald ripening and thus allows the coexistence of multiple pyrenoids instead of fusing into one as observed in *Chlamydomonas* [36, 44]. In many species the pyrenoid is localized centrally in the chloroplast amidst the thylakoids (common in glaucophytes and all green lineages; some rhodophytes and diatoms), in other species the pyrenoid is localized in peripheral protrusions of the chloroplast (common in all TSAR lineages and some rhodophytes). In species with a peripheral pyrenoid the pyrenoid is tightly encircled by the chloroplast envelope and the protrusion is typically into the central cytosolic space. In many species the pyrenoid is traversed by one or more membrane tubules that typically are continuous with the thylakoid membrane (for clarity, in the following we term these thylakoid tubules) but can be derived from other cellular membranes, collectively these are termed pyrenoid tubules. The thylakoid tubules are presumably important for the delivery of inorganic carbon as discussed above for *Chlamydomonas* and postulated in the diatom *Phaeodactylum tricornutum*, whose single pyrenoid tubule contains a carbonic anhydrase [244]. Observations across lineages indicate that thylakoid tubules are biochemically distinct from other parts of the thylakoid membrane. Thylakoid tubules across lineages typically lack active PSII, which would produce O_2 in close proximity to Rubisco and thus promote the oxygenase function of Rubisco, reducing photosynthetic performance [55, 88, 117, 118].

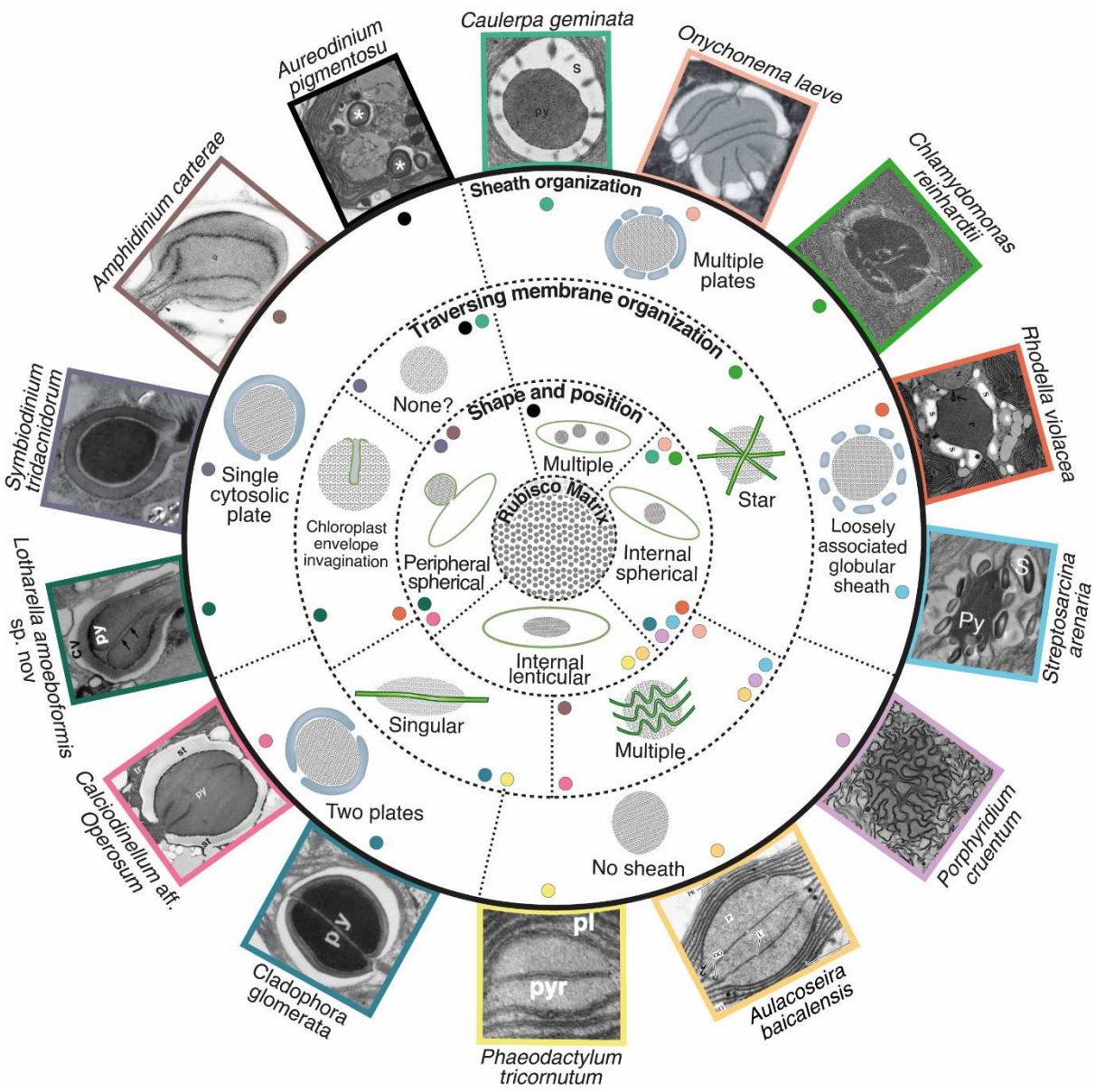

Figure 6. Pyrenoids are structurally diverse. Peripheral TEM images are used to demonstrate non-exhaustive examples of combinations of pyrenoid structural features. Starting centrally, with the defining pyrenoid matrix and radiating outwards, combinations of matrix shape/position, traversing membrane organization and sheath organization can be achieved. Observed combinations are loosely demarcated by dashed lines between and within rings, but no combinations are definitively excluded. Coloured dots indicate combinations of structural features, corresponding to image borders. Image labelling is from original publication: p/py/pyr/*, pyrenoid; s/st, starch; pl, plastid; cv, capping vesicle. References for images, clockwise from *Caulerpa geminata* [245], *Onchynonema laeve* [100], *Chlamydomonas reinhardtii* (authors collection), *Rhodella violacea* [246], *Streptosarcina arenaria* [247], *Porphyridium cruentum* [55], *Aulacoseira baicalensis* [248], *Phaeodactylum tricornutum* [249], *Cladophora glomerata* [250], *Calciodinellum* aff. *Operosum* [60], *Lotharella amoeboformis* sp. nov [251], *Symbiodinium tridacnidorum* [252], *Amphidinium carterae* [148], *Aureodinium pigmentosu* [253].

Although it is currently assumed that the thylakoid tubules are important for the delivery of inorganic carbon to the pyrenoid, not all pyrenoid containing species have a matrix traversed

by thylakoid tubules. Thylakoid tubules are seen in all hornwort pyrenoids and there are example species in all algal lineages except for glaucophytes. With data in many species limited to a handful of TEM images, it is possible that TEM sectioning could fail to reveal tubules. In species with peripheral pyrenoids the thylakoid tubules are often missing. In these species, the thylakoid membrane often stops before the pyrenoid matrix begins [131, 246, 254, 255] and, in some cases, the thylakoid tips extend into the matrix [256]. However, there are exceptions (e.g. dinophytes), where thylakoid tubules cross the matrix of peripheral pyrenoids completely or even form networks in them [60, 257]. In species with peripheral pyrenoids without thylakoid tubules, the chloroplast envelope can extend into the pyrenoid matrix by forming tubular intrusions, indicating that membranes traversing the pyrenoid is potentially a ubiquitous feature. In striking examples of such envelope intrusions, the internal region of the pyrenoid seems to be directly connected to the cytosol, nucleus or mitochondria. The nuclear envelope of the rhodophyte *Rhodella violacea* is in direct contact with the chloroplast and elongation of the nuclear envelope into the pyrenoid at a chloroplast envelope intrusion suggests interaction between the nucleus and the pyrenoid [246]. In the chlorophyte *Prasinoderma singularis* it is claimed that the mitochondria protrudes through the chloroplast envelope intrusion into the pyrenoid [258], opening the possibility that photorespiratory CO_2 release could directly be driving photosynthetic carbon fixation. The function of all pyrenoid traversing chloroplast envelope intrusions remain unknown, but it seems likely that they are also involved in CO_2 delivery to the pyrenoid.

The characteristics and complexity of pyrenoid tubules varies greatly between species (Figure 6). Tubules have been used as taxonomic markers in some lineages (e.g. in dinophytes [259] or diatoms [248]). The least complex examples are where the pyrenoid is traversed only by a single thylakoid tubule, which is found in some chlorophytes and diatoms [248, 260, 261]. In several chlorophyte, dinophyte and euglenophyte species the pyrenoid is traversed by multiple non-connecting parallel membranes [248, 261-263]. Other species form more or less complex, interconnected thylakoid tubule networks within the pyrenoid matrix, which is common in chlorophyte, rhodophyte and hornwort species. Some species like *Chlamydomonas* have relatively simple star-shaped (2D view or stellate as seen in 3D) thylakoid tubule networks crossing their pyrenoid, whilst other species like the rhodophyte *Porphyridium cruentum* [127, 129], the chlorophyte genus *Zygnema* [264-266] or hornworts [50] show highly complex networks of interconnected tubules. The thylakoid tubules can drastically differ from the rest of the thylakoid network as stacked membranes usually unstack and enter the pyrenoid as single entities or merge and enter the pyrenoid as composites. However, in other species the thylakoid membrane appears not to change as it enters the pyrenoid matrix, for instance the hornwort genus *Dendroceros* maintains even grana stacks in the pyrenoid matrix [50].

Even though different algal lineages use different carbohydrates for energy storage, there are example species from all algal clades that surround their pyrenoid with a layer of their storage material (hereafter referred to as starch sheath). This is even more astonishing considering that rhodophytes and algal lineages that inherited a “red” chloroplast through secondary endosymbiosis store their reserve material not in the chloroplast but in the cytosol. Consequently, only peripheral pyrenoids in “red” chloroplasts exhibit a starch sheath and central pyrenoids are always sheath-less in these lineages. Glaucophytes never have a starch sheath, and in the green lineages the pyrenoid is often, but not always, surrounded by a starch sheath. The morphology of the starch sheath varies greatly between species (Figure 6). The starch sheath can be formed by only one plate [254, 267, 268] and in species, where the pyrenoid matrix is crossed by a single thylakoid disc, the starch sheath is sometimes formed

by two plates [250, 269], but in most cases the starch sheath is formed by several plates. In some species there are broad gaps between the starch plates [62, 246, 247], whereas in others the plates sit tightly together, sometimes even in multiple layers [270]. The starch sheath has been posited to function as a structural barrier that prevents CO_2 leakage from the pyrenoid, with some supporting evidence for this in *Chlamydomonas* [42, 73, 91].

Differences in pyrenoid structure across algae indicates that inorganic carbon flow from the external environment to Rubisco must differ from the described mechanism for *Chlamydomonas*. In species with pyrenoids lacking thylakoid tubules, inorganic carbon must enter the pyrenoid matrix directly from the chloroplast stroma without entering the thylakoid lumen or even from the cytosol in the case of peripheral pyrenoids without even entering the chloroplast stroma, perhaps through chloroplast envelope intrusions that extend into the pyrenoid matrix. Species without a starch sheath around the pyrenoid potentially lose more CO_2 through leaking than species with a starch sheath. However, the presence of low electron dense CO_2 impermeable protein layers or membrane diffusion barriers created from adjacent thylakoids or the chloroplast envelope cannot be ruled out.

Outside of *Chlamydomonas*, we currently lack a molecular understanding of the structural arrangement of the pyrenoid across algal lineages and hornworts) and, consequently, mostly understand the operation of these CCMs by analogy to *Chlamydomonas*. Thus, it will be key to obtain information on the structure and function of pyrenoids from other algae as well as from hornworts in order to fully understand the principles of CCM function, which is pivotal for any engineering approaches into crop plants. Moreover, a deeper knowledge of the pyrenoid structure and function of ecologically relevant algae, such as diatoms and coccolithophores, will help to better understand global carbon flows.

SYNTHETIC PYRENOID ASSEMBLY AND RELEVANCE TO HIGHER PLANT ENGINEERING

In modern agriculture where biotic and abiotic stresses such as water and nitrogen availability, pests and pathogens can be controlled, crop yield can become limited by CO_2 fixation by photosynthesis [271]. Calculations show that many C_3 crops, such as rice, wheat and soya are only reaching at maximum one-third of their theoretical potential of conversion of solar energy capture to carbohydrate synthesis [272]. It is thought that photosynthetic performance has not been selected for through breeding programmes due to it being highly conserved within crop species giving very little room for positive selection [17]. A promising strategy for photosynthetic improvements is the engineering of a CCM (see [201, 273-275] for recent detailed reviews). Modelling has shown that biophysical CCM engineering in the form of a pyrenoid or carboxysome centred CCM could result in theoretical yield increases of 60% along with improvements in water and nitrogen use efficiencies [17, 276]. However, predicting yield increases from photosynthetic improvements is complicated due to the complex interplay of multiple processes that determine crop yield. This has been demonstrated by cross-scale modelling that indicate that simultaneous improvements in Rubisco activity (i.e. CCM presence), electron transport and mesophyll conductance maybe required for significant yield improvements [277]. Field data in tobacco supports photosynthetic engineering as a promising approach with significant increases in plant biomass seen with multiple approaches, including synthetic photorespiratory bypasses to reduce photorespiration [278], enhanced photoprotection [279] and combined improvements in RuBP regeneration and electron transport [280]. Although, how biomass improvements will translate to grain crop yields is unclear. The potential for increasing CO_2 supply to Rubisco through CCM engineering to

translate into grain yield improvements is supported to some extent by in field data where season-long CO_2 enrichment using free-air concentration enrichment (FACE) technology has demonstrated yield improvements on average of 17% across rice, wheat, cotton and sorghum [271].

Algal CCM engineering is currently underway with successful expression of multiple CCM components that correctly localize in Arabidopsis [281]. To prime plants for pyrenoid assembly via EPYC1, Arabidopsis lines that have had the majority of their native Rubisco SSU replaced with *Chlamydomonas* Rubisco SSU have been developed and the hybrid Rubisco shown to be functional [282]. Purified Arabidopsis/ *Chlamydomonas* hybrid Rubisco has then been shown to undergo LLPS *in vitro* [97]. Optimised EPYC1 expression in Arabidopsis expressing *Chlamydomonas* Rubisco SSU has recently resulted in *in planta* proto-pyrenoid assembly (i.e. EPYC1/ Rubisco condensation) [283], with Arabidopsis proto-pyrenoids having a comparable size and internal mixing to *Chlamydomonas* pyrenoids [36, 283]. In contrast to *in planta* carboxysome assembly where Rubisco packaging results in severely reduced plant growth [284], proto-pyrenoid expressing lines have a similar photosynthetic performance to wild-type [283]. Although plant proto-pyrenoid assembly is a major breakthrough, photosynthetic improvements most likely will only be realized once a complete CCM is assembled. Based on conserved structural features of pyrenoids across algae and our current knowledge of the CCM, a minimum CCM is expected to require: 1) Rubisco/EPYC1 matrix assembly around thylakoids; 2) inorganic carbon delivery to the matrix traversing thylakoids via HCO_3^- channels; and 3) accelerated dehydration of HCO_3^- to CO_2 via a carbonic anhydrase localized in the matrix traversing thylakoids. Further pyrenoid structural refinements may include modification of thylakoids traversing the pyrenoid matrix, similar to pyrenoid tubule assemblies observed in *Chlamydomonas*; the assembly of a pyrenoid starch sheath to minimise CO_2 retro diffusion out of the pyrenoid; and additional inorganic carbon accumulation systems at the chloroplast envelope (i.e. LCIA) and the pyrenoid periphery (i.e. LCIB/LCIC complex). In addition, detailed understanding and engineering control of pyrenoid assembly, regulation and division within different plant leaf cell-types will be critical for successful function. Understanding pyrenoid assembly across diverse algae will offer additional approaches to engineering plants with pyrenoid CCMs. Moreover, it will also open opportunities for hybrid assemblies and the development of synthetic/designer parts. A primary example could be the development of synthetic EPYC1 analogues that can phase separate plant Rubisco removing the requirement to modify plant Rubisco SSU.

SUMMARY

The pyrenoid is a biogeochemically important organelle central to biophysical CCMs that contribute massively to photosynthetic primary production and offer serious prospect for enhancing crop yields. Once considered amorphous/crystalline, recent work has allowed characterization of the *Chlamydomonas* pyrenoid as a LLPS body, formed by complex coacervation between Rubisco and a disordered linker protein, EPYC1. The liquid-like properties of the pyrenoid play a critical role in ensuring robust pyrenoid inheritance and most likely enable rapid adaption of carbon fixation through the CBB cycle in response to changes in inorganic carbon and light availability. The commonality of pyrenoid dynamics, ultrastructural features and putative Rubisco linkers described across the eukaryotic tree of life suggest that LLPS may be common to the functionality of pyrenoids, however conclusive evidence across diverse phyla is currently lacking. Despite rapid recent advances in our

understanding of the *Chlamydomonas* pyrenoid as a LLPS organelle, key gaps in our knowledge exist. We are only beginning to understand the basis of the molecular structure that underpins the defining macroscopic properties and ultrastructural arrangements exhibited by pyrenoids. Understanding the molecular basis for phase separation will facilitate an understanding of the processes that determine the dynamic transitions of the pyrenoid, most likely essential to its adaptive function across lineages. Additionally, understanding the role of ultrastructural features and their associated molecular factors in pyrenoid assembly, localization and division will be central to understanding the underlying properties for pyrenoid function. This understanding will have direct implications for the rapidly evolving efforts to introduce pyrenoids into higher plants, that have been somewhat retarded by key gaps in our knowledge. From a molecular scale to global impact, extending our in-depth knowledge of pyrenoid function to diverse and globally important pyrenoid-containing lineages will facilitate our understanding of how/if Rubisco LLPS has driven the complex evolutionary history of the pyrenoid and provide molecular level biophysical based principles that underly ~30% of global carbon fixation.

ACKNOWLEDGEMENTS

We would like to thank the support and constructive comments from Avi Flamholz, Moritz Meyer, Ursula Goodenough, Martin Jonikas, Alistair McCormick, Nicky Atkinson, Liat Adler, Aranzazú Díaz Ramos, Charlotte Walker and Eleanor Fletcher whose input dramatically improved the review. The review was supported by funding from UK Biotechnology and Biological Sciences Research Council (BBSRC) Grants BB/R001014/1 and BB/S015337/1 (to LCMM); Leverhulme Trust Grant RPG-2017-402 (to LCMM); UK Research and Innovation Future Leader Fellowship MR/T020679/1 (to LCMM) and BBSRC DTP2 BB/M011151/1a (to JB and LCMM).

REFERENCES

[1] C.B. Field, M.J. Behrenfeld, J.T. Randerson, P. Falkowski, Primary production of the biosphere: integrating terrestrial and oceanic components, Science, 281 (1998) 237-240.
[2] A. Bar-Even, E. Noor, Y. Savir, W. Liebermeister, D. Davidi, D.S. Tawfik, R. Milo, The Moderately Efficient Enzyme: Evolutionary and Physicochemical Trends Shaping Enzyme Parameters, Biochemistry, 50 (2011) 4402-4410.
[3] S.M. Whitney, R.L. Houtz, H. Alonso, Advancing our understanding and capacity to engineer nature's CO_2-sequestering enzyme, Rubisco, Plant Physiol., 155 (2011) 27-35.
[4] G.G.B. Tcherkez, G.D. Farquhar, T.J. Andrews, Despite slow catalysis and confused substrate specificity, all ribulose bisphosphate carboxylases may be nearly perfectly optimized, Proceedings of the National Academy of Sciences, 103 (2006) 7246-7251.
[5] R.A. Studer, P.-A. Christin, M.A. Williams, C.A. Orengo, Stability-activity tradeoffs constrain the adaptive evolution of RubisCO, Proceedings of the National Academy of Sciences, 111 (2014) 2223-2228.
[6] A.I. Flamholz, N. Prywes, U. Moran, D. Davidi, Y.M. Bar-On, L.M. Oltrogge, R. Alves, D. Savage, R. Milo, Revisiting Trade-offs between Rubisco Kinetic Parameters, Biochemistry, 58 (2019) 3365-3376.
[7] J. Galmés, M.V. Kapralov, P.J. Andralojc, M.À. Conesa, A.J. Keys, M.A.J. Parry, J. Flexas, Expanding knowledge of the Rubisco kinetics variability in plant species: environmental and evolutionary trends, Plant, Cell & Environment, 37 (2014) 1989-2001.
[8] R.J. Ellis, The most abundant protein in the world, Trends Biochem. Sci., 4 (1979) 241-244.

[9] J.A. Raven, Rubisco: still the most abundant protein of Earth?, New Phytol., 198 (2013) 1-3.
[10] G.D. Price, M.R. Badger, Expression of Human Carbonic Anhydrase in the Cyanobacterium *Synechococcus* PCC7942 Creates a High CO_2-Requiring Phenotype Evidence for a Central Role for Carboxysomes in the CO_2 Concentrating Mechanism, Plant Physiol., 91 (1989) 505-513.
[11] J. Karlsson, A.K. Clarke, Z.Y. Chen, S.Y. Hugghins, Y.I. Park, H.D. Husic, J.V. Moroney, G. Samuelsson, A novel alpha-type carbonic anhydrase associated with the thylakoid membrane in *Chlamydomonas reinhardtii* is required for growth at ambient CO_2, EMBO J., 17 (1998) 1208-1216.
[12] N.M. Mangan, A. Flamholz, R.D. Hood, R. Milo, D.F. Savage, pH determines the energetic efficiency of the cyanobacterial CO_2 concentrating mechanism, Proc. Natl. Acad. Sci. U. S. A., 113 (2016) E5354-5362.
[13] A. Flamholz, P.M. Shih, Cell biology of photosynthesis over geologic time, Current Biology, 30 (2020) R490-R494.
[14] B.D. Rae, B.M. Long, M.R. Badger, G.D. Price, Functions, compositions, and evolution of the two types of carboxysomes: polyhedral microcompartments that facilitate CO_2 fixation in cyanobacteria and some proteobacteria, Microbiol. Mol. Biol. Rev., 77 (2013) 357-379.
[15] M.T. Meyer, M.M.M. Goudet, H. Griffiths, The Algal Pyrenoid, in: A.W.D. Larkum, A.R. Grossmann, J.A. Raven (Eds.) Photosynthesis in Algae: Biochemical and Physiological Mechanisms, Springer International Publishing, Place Published, 2020, pp. 179-203.
[16] J.A. Raven, The possible roles of algae in restricting the increase in atmospheric CO_2 and global temperature, Eur. J. Phycol., 52 (2017) 506-522.
[17] S.P. Long, S. Burgess, I. Causton, Redesigning crop photosynthesis, in: R. Zeigler (Ed.) Sustaining Global Food Security: The Nexus of Science and Policy, CSIRO Publishing, Place Published, 2019, pp. 128-147.
[18] D.K. Ray, N.D. Mueller, P.C. West, J.A. Foley, Yield trends are insufficient to double global crop production by 2050, PLoS One, 8 (2013) e66428.
[19] S. Alberti, Phase separation in biology, Curr. Biol., 27 (2017) R1097-R1102.
[20] S. Boeynaems, S. Alberti, N.L. Fawzi, T. Mittag, M. Polymenidou, F. Rousseau, J. Schymkowitz, J. Shorter, B. Wolozin, L. Van Den Bosch, P. Tompa, M. Fuxreiter, Protein Phase Separation: A New Phase in Cell Biology, Trends Cell Biol., 28 (2018) 420-435.
[21] P. Li, S. Banjade, H.-C. Cheng, S. Kim, B. Chen, L. Guo, M. Llaguno, J.V. Hollingsworth, D.S. King, S.F. Banani, P.S. Russo, Q.-X. Jiang, B.T. Nixon, M.K. Rosen, Phase transitions in the assembly of multivalent signalling proteins, Nature, 483 (2012) 336-340.
[22] S.F. Banani, H.O. Lee, A.A. Hyman, M.K. Rosen, Biomolecular condensates: organizers of cellular biochemistry, Nat. Rev. Mol. Cell Biol., 18 (2017) 285-298.
[23] J.-P. Vaucher, Histoire des conferves d'eau douce, contenant leurs différens modes de reproduction, et la description de leurs principales espèces, suivie de l'histoire des trémelles et des ulves d'eau douce. Par Jean-Pierre Vaucher, Place Published, 1803.
[24] C.P. Brangwynne, C.R. Eckmann, D.S. Courson, A. Rybarska, C. Hoege, J. Gharakhani, F. Jülicher, A.A. Hyman, Germline P granules are liquid droplets that localize by controlled dissolution/condensation, Science, 324 (2009) 1729-1732.
[25] A.A. Hyman, C.A. Weber, F. Julicher, Liquid-liquid phase separation in biology, Annu. Rev. Cell Dev. Biol., 30 (2014) 39-58.
[26] K.A. Rosowski, T. Sai, E. Vidal-Henriquez, D. Zwicker, R.W. Style, E.R. Dufresne, Elastic ripening and inhibition of liquid-liquid phase separation, Nat. Phys., 16 (2020) 422-425.
[27] D.T. McSwiggen, M. Mir, X. Darzacq, R. Tjian, Evaluating phase separation in live cells: diagnosis, caveats, and functional consequences, Genes Dev., 33 (2019) 1619-1634.
[28] C.L. Cuevas-Velazquez, J.R. Dinneny, Organization out of disorder: liquid-liquid phase separation in plants, Curr. Opin. Plant Biol., 45 (2018) 68-74.
[29] D.M. Mitrea, R.W. Kriwacki, Phase separation in biology; functional organization of a higher order, Cell Commun. Signal., 14 (2016) 1.

[30] G.L. Dignon, R.B. Best, J. Mittal, Biomolecular Phase Separation: From Molecular Driving Forces to Macroscopic Properties, Annu. Rev. Phys. Chem., 71 (2020) 53-75.
[31] I. Peran, T. Mittag, Molecular structure in biomolecular condensates, Curr. Opin. Struct. Biol., 60 (2020) 17-26.
[32] J.-M. Choi, R.V. Pappu, The Stickers and Spacers Framework for Describing Phase Behavior of Multivalent Intrinsically Disordered Proteins, Biophys. J., 118 (2020) 492a.
[33] J.-M. Choi, A.S. Holehouse, R.V. Pappu, Physical Principles Underlying the Complex Biology of Intracellular Phase Transitions, Annu. Rev. Biophys., 49 (2020) 107-133.
[34] S.F. Banani, A.M. Rice, W.B. Peeples, Y. Lin, S. Jain, R. Parker, M.K. Rosen, Compositional Control of Phase-Separated Cellular Bodies, Cell, 166 (2016) 651-663.
[35] I. Owen, F. Shewmaker, The Role of Post-Translational Modifications in the Phase Transitions of Intrinsically Disordered Proteins, Int. J. Mol. Sci., 20 (2019) 5501.
[36] E.S. Freeman Rosenzweig, B. Xu, L. Kuhn Cuellar, A. Martinez-Sanchez, M. Schaffer, M. Strauss, H.N. Cartwright, P. Ronceray, J.M. Plitzko, F. Förster, N.S. Wingreen, B.D. Engel, L.C.M. Mackinder, M.C. Jonikas, The Eukaryotic CO_2-Concentrating Organelle Is Liquid-like and Exhibits Dynamic Reorganization, Cell, 171 (2017) 148-162.e119.
[37] M. Feric, C.P. Brangwynne, A nuclear F-actin scaffold stabilizes ribonucleoprotein droplets against gravity in large cells, Nat. Cell Biol., 15 (2013) 1253-1259.
[38] S. Elbaum-Garfinkle, Y. Kim, K. Szczepaniak, C.C.-H. Chen, C.R. Eckmann, S. Myong, C.P. Brangwynne, The disordered P granule protein LAF-1 drives phase separation into droplets with tunable viscosity and dynamics, Proc. Natl. Acad. Sci. U. S. A., 112 (2015) 7189-7194.
[39] K.Y. Han, L. Graf, C.P. Reyes, B. Melkonian, R.A. Andersen, H.S. Yoon, M. Melkonian, A Re-investigation of *Sarcinochrysis marina* (Sarcinochrysidales, Pelagophyceae) from its Type Locality and the Descriptions of *Arachnochrysis*, *Pelagospilus*, *Sargassococcus* and *Sungminbooa* genera nov, Protist, 169 (2018) 79-106.
[40] M.-T. Wei, S. Elbaum-Garfinkle, A.S. Holehouse, C.C.-H. Chen, M. Feric, C.B. Arnold, R.D. Priestley, R.V. Pappu, C.P. Brangwynne, Phase behaviour of disordered proteins underlying low density and high permeability of liquid organelles, Nat. Chem., 9 (2017) 1118-1125.
[41] T.S. Harmon, A.S. Holehouse, M.K. Rosen, R.V. Pappu, Intrinsically disordered linkers determine the interplay between phase separation and gelation in multivalent proteins, Elife, 6 (2017) e30294.
[42] A.K. Itakura, K.X. Chan, N. Atkinson, L. Pallesen, L. Wang, G. Reeves, W. Patena, O. Caspari, R. Roth, U. Goodenough, A.J. McCormick, H. Griffiths, M.C. Jonikas, A Rubisco-binding protein is required for normal pyrenoid number and starch sheath morphology in *Chlamydomonas reinhardtii*, Proc. Natl. Acad. Sci. U. S. A., 116 (2019) 18445-18454.
[43] L.M. Oltrogge, T. Chaijarasphong, A.W. Chen, E.R. Bolin, S. Marqusee, D.F. Savage, Multivalent interactions between CsoS2 and Rubisco mediate α-carboxysome formation, Nat. Struct. Mol. Biol., 27 (2020) 281-287.
[44] T. Wunder, S.L.H. Cheng, S.-K. Lai, H.-Y. Li, O. Mueller-Cajar, The phase separation underlying the pyrenoid-based microalgal Rubisco supercharger, Nat. Commun., 9 (2018) 5076.
[45] M. Ludwig, D. Sültemeyer, G.D. Price, Isolation of *ccm*KLMN genes from the marine cyanobacterium, *Synechococcus* sp. PCC7002 (Cyanophyceae), and evidence that CcmM is essential for carboxysome assembly, J. Phycol., 36 (2000) 1109-1119.
[46] F. Cai, Z. Dou, S.L. Bernstein, R. Leverenz, E.B. Williams, S. Heinhorst, J. Shively, G.C. Cannon, C.A. Kerfeld, Advances in Understanding Carboxysome Assembly in *Prochlorococcus* and *Synechococcus* Implicate CsoS2 as a Critical Component, Life, 5 (2015) 1141-1171.
[47] H. Wang, X. Yan, H. Aigner, A. Bracher, N.D. Nguyen, W.Y. Hee, B.M. Long, G.D. Price, F.U. Hartl, M. Hayer-Hartl, Rubisco condensate formation by CcmM in β-carboxysome biogenesis, Nature, 566 (2019) 131-135.

[48] A.H. Chen, A. Robinson-Mosher, D.F. Savage, P.A. Silver, J.K. Polka, The bacterial carbon-fixing organelle is formed by shell envelopment of preassembled cargo, PLoS One, 8 (2013) e76127.
[49] C.A. Kerfeld, M.R. Melnicki, Assembly, function and evolution of cyanobacterial carboxysomes, Current Opinion in Plant Biology, 31 (2016) 66-75.
[50] J.C. Villarreal, S.S. Renner, Hornwort pyrenoids, carbon-concentrating structures, evolved and were lost at least five times during the last 100 million years, Proc. Natl. Acad. Sci. U. S. A., 109 (2012) 18873-18878.
[51] L.C.M. Mackinder, M.T. Meyer, T. Mettler-Altmann, V.K. Chen, M.C. Mitchell, O. Caspari, E.S. Freeman Rosenzweig, L. Pallesen, G. Reeves, A. Itakura, R. Roth, F. Sommer, S. Geimer, T. Mühlhaus, M. Schroda, U. Goodenough, M. Stitt, H. Griffiths, M.C. Jonikas, A repeat protein links Rubisco to form the eukaryotic carbon-concentrating organelle, Proc. Natl. Acad. Sci. U. S. A., 113 (2016) 5958-5963.
[52] M.D. Guiry, How Many Species of Algae Are There?, J. Phycol., 48 (2012) 1057-1063.
[53] F. Burki, A.J. Roger, M.W. Brown, A.G.B. Simpson, The New Tree of Eukaryotes, Trends Ecol. Evol., 35 (2020) 43-55.
[54] M. Sato, Y. Mogi, T. Nishikawa, S. Miyamura, T. Nagumo, S. Kawano, The dynamic surface of dividing cyanelles and ultrastructure of the region directly below the surface in *Cyanophora paradoxa*, Planta, 229 (2009) 781.
[55] R.M. McKay, S.P. Gibbs, Phycoerythrin is absent from the pyrenoid of *Porphyridium cruentum*: photosynthetic implications, Planta, 180 (1990) 249-256.
[56] I. Ohad, P. Siekevitz, G.E. Palade, Biogenesis of chloroplast membranes. I. Plastid dedifferentiation in a dark-grown algal mutant (*Chlamydomonas reinhardi*), J. Cell Biol., 35 (1967) 521-552.
[57] F.W. Li, J.C. Villarreal, P. Szovenyi, Hornworts: An Overlooked Window into Carbon-Concentrating Mechanisms, Trends Plant Sci., 22 (2017) 275-277.
[58] P.L. Walne, H.J. Arnott, The comparative ultrastructure and possible function of eyespots: *Euglena granulata* and *Chlamydomonas eugametos*, Planta, 77 (1967) 325-353.
[59] M. Tachibana, A.E. Allen, S. Kikutani, Y. Endo, C. Bowler, Y. Matsuda, Localization of putative carbonic anhydrases in two marine diatoms, *Phaeodactylum tricornutum* and *Thalassiosira pseudonana*, Photosynth. Res., 109 (2011) 205-221.
[60] C. Zinssmeister, H. Keupp, G. Tischendorf, F. Kaulbars, M. Gottschling, Ultrastructure of calcareous dinophytes (Thoracosphaeraceae, Peridiniales) with a focus on vacuolar crystal-like particles, PLoS One, 8 (2013) e54038.
[61] S. Ota, K. Ueda, K.-I. Ishida, *Lotharella vacuolata* sp. nov., a new species of chlorarachniophyte algae, and time-lapse video observations on its unique post-cell division behavior, Phycological Res., 53 (2005) 275-286.
[62] S.W. Nam, D. Go, M. Son, W. Shin, Ultrastructure of the flagellar apparatus in *Rhinomonas reticulata* var. atrorosea (Cryptophyceae, Cryptophyta), Algae, 28 (2013) 331-341.
[63] A.W.F. Schimper, Untersuchungen über die Chlorophyllkörper und die ihnen homologen Gebilde, Jahrb. wiss. Bot, 16 (1885) 1-247.
[64] R. Wagner, Einige bemerkungen und fragen über das keimbläschen (vesicular germinativa), Müller's Archiv Anat Physiol Wissenschaft Med, 268 (1835) 373-377.
[65] F. Schmitz, Die chromatophoren der algen: Vergleichende untersuchungen über bau und entwicklung der chlorophyllkörper und der analogen farbstoffkörper der algen, M. Cohen & Sohn (F. Cohen), Place Published, 1882.
[66] R.H. Holdsworth, The isolation and partial characterization of the pyrenoid protein of *Eremosphaera viridis*, J. Cell Biol., 51 (1971) 499-513.
[67] U.W. Goodenough, R. Levine, Chloroplast structure and function in ac-20, a mutant strain of *Chlamydomonas reinhardi*. 3. Chloroplast ribosomes and membrane organization, J. Cell Biol., 44 (1970) 547-562.
[68] N.W. Kerby, L.V. Evans, Isolation and partial characterization of pyrenoids from the brown alga Pilayella littoralis (L.) Kjellm, Planta, 142 (1978) 91-95.

[69] J.L. Salisbury, G.L. Floyd, Molecular, enzymatic and ultrastructure characterization of the scaly green monad *Micromonas squamata*, Journal of Phycology, 14 (1978) 362-368.
[70] G. Lacoste-Royal, S.P. Gibbs, Immunocytochemical localization of ribulose-1, 5-bisphosphate carboxylase in the pyrenoid and thylakoid region of the chloroplast of *Chlamydomonas reinhardtii*, Plant Physiology, 83 (1987) 602-606.
[71] M.G. Vladimirova, A.G. Markelova, V.E. Semenenko, Use of the cytoimmunofluorescent method to clarify localization of ribulose bisphosphate carboxylase in pyrenoids of unicellular algae, Fiziol Rast, 29 (1982) 725-734.
[72] K. Kuchitsu, M. Tsuzuki, S. Miyachi, Polypeptide composition and enzyme activities of the pyrenoid and its regulation by CO_2 concentration in unicellular green algae, Can. J. Bot., 69 (1991) 1062-1069.
[73] Z. Ramazanov, M. Rawat, M.C. Henk, C.B. Mason, S.W. Matthews, J.V. Moroney, The induction of the CO_2-concentrating mechanism is correlated with the formation of the starch sheath around the pyrenoid of *Chlamydomonas reinhardtii*, Planta, 195 (1994) 210–216.
[74] K. Palmqvist, Photosynthetic CO_2-use efficiency in lichens and their isolated photobionts: the possible role of a CO_2-concentrating mechanism, Planta, 191 (1993) 48-56.
[75] M.R. Badger, H. Pfanz, B. Büdel, U. Heber, O.L. Lange, Evidence for the functioning of photosynthetic CO_2-concentrating mechanisms in lichens containing green algal and cyanobacterial photobionts, Planta, 191 (1993) 57-70.
[76] P.-A. Dangeard, Recherches sur les algues inférieures, Ann Sci Nat Bot Ser VII, 7 (1888) 105-175.
[77] M.T. Meyer, C. Whittaker, H. Griffiths, The algal pyrenoid: key unanswered questions, J. Exp. Bot., 68 (2017) 3739-3749.
[78] P.A. Salomé, S.S. Merchant, A Series of Fortunate Events: Introducing *Chlamydomonas* as a Reference Organism, Plant Cell, 31 (2019) 1682–1707.
[79] B.D. Engel, M. Schaffer, L. Kuhn Cuellar, E. Villa, J.M. Plitzko, W. Baumeister, Native architecture of the *Chlamydomonas* chloroplast revealed by in situ cryo-electron tomography, Elife, 4 (2015) e04889.
[80] L.C.M. Mackinder, C. Chen, R.D. Leib, W. Patena, S.R. Blum, M. Rodman, S. Ramundo, C.M. Adams, M.C. Jonikas, A Spatial Interactome Reveals the Protein Organization of the Algal CO_2-Concentrating Mechanism, Cell, 171 (2017) 133-147.e114.
[81] Y. Zhan, C.H. Marchand, A. Maes, A. Mauries, Y. Sun, J.S. Dhaliwal, J. Uniacke, S. Arragain, H. Jiang, N.D. Gold, V.J.J. Martin, S.D. Lemaire, W. Zerges, Pyrenoid functions revealed by proteomics in *Chlamydomonas* reinhardtii, PLoS One, 13 (2018) e0185039.
[82] A. Küken, F. Sommer, L. Yaneva-Roder, L.C. Mackinder, M. Höhne, S. Geimer, M.C. Jonikas, M. Schroda, M. Stitt, Z. Nikoloski, T. Mettler-Altmann, Effects of microcompartmentation on flux distribution and metabolic pools in *Chlamydomonas reinhardtii* chloroplasts, Elife, 7 (2018) e37960.
[83] W. Wietrzynski, M. Schaffer, D. Tegunov, S. Albert, A. Kanazawa, J.M. Plitzko, W. Baumeister, B.D. Engel, Charting the native architecture of *Chlamydomonas* thylakoid membranes with single-molecule precision, Elife, 9 (2020) e53740.
[84] A. Mukherjee, C.S. Lau, C.E. Walker, A.K. Rai, C.I. Prejean, G. Yates, T. Emrich-Mills, S.G. Lemoine, D.J. Vinyard, L.C.M. Mackinder, J.V. Moroney, Thylakoid localized bestrophin-like proteins are essential for the CO_2 concentrating mechanism of *Chlamydomonas reinhardtii*, Proc. Natl. Acad. Sci. U. S. A., 116 (2019) 16915-16920.
[85] M. Mitra, S.M. Lato, R.A. Ynalvez, Y. Xiao, J.V. Moroney, Identification of a new chloroplast carbonic anhydrase in *Chlamydomonas reinhardtii*, Plant Physiol., 135 (2004) 173-182.
[86] D. Duanmu, Y. Wang, M.H. Spalding, Thylakoid lumen carbonic anhydrase (CAH3) mutation suppresses air-Dier phenotype of LCIB mutant in *Chlamydomonas reinhardtii*, Plant Physiol., 149 (2009) 929-937.
[87] M.A. Sinetova, E.V. Kupriyanova, A.G. Markelova, S.I. Allakhverdiev, N.A. Pronina, Identification and functional role of the carbonic anhydrase Cah3 in thylakoid membranes of pyrenoid of *Chlamydomonas reinhardtii*, Biochim. Biophys. Acta, 1817 (2012) 1248-1255.

[88] R.M.L. McKay, S.P. Gibbs, Composition and function of pyrenoids: cytochemical and immunocytochemical approaches, Can. J. Bot., 69 (1991) 1040-1052.
[89] K. Kuchitsu, M. Tsuzuki, S. Miyachi, Changes of Starch Localization within the Chloroplast Induced by Changes in CO_2 Concentration during Growth of *Chlamydomonas reinhardtii*: Independent Regulation of Pyrenoid Starch and Stroma Starch, Plant Cell Physiol., 29 (1988) 1269-1278.
[90] A. Villarejo, F. Martinez, M. Pino Plumed, Z. Ramazanov, The induction of the CO_2 concentrating mechanism in a starch-less mutant of *Chlamydomonas reinhardtii*, Physiol. Plant., 98 (1996) 798-802.
[91] C. Toyokawa, T. Yamano, H. Fukuzawa, Pyrenoid Starch Sheath Is Required for LCIB Localization and the CO_2-Concentrating Mechanism in Green Algae, Plant Physiol., 182 (2020) 1883-1893.
[92] T. Yamano, T. Tsujikawa, K. Hatano, S.-I. Ozawa, Y. Takahashi, H. Fukuzawa, Light and Low-CO_2-Dependent LCIB–LCIC Complex Localization in the Chloroplast Supports the Carbon-Concentrating Mechanism in *Chlamydomonas reinhardtii*, Plant Cell Physiol., 51 (2010) 1453-1468.
[93] Y. Wang, D.J. Stessman, M.H. Spalding, The CO_2 concentrating mechanism and photosynthetic carbon assimilation in limiting CO_2: how *Chlamydomonas* works against the gradient, Plant J., 82 (2015) 429–448.
[94] S. Jin, J. Sun, T. Wunder, D. Tang, A.B. Cousins, S.K. Sze, O. Mueller-Cajar, Y.-G. Gao, Structural insights into the LCIB protein family reveals a new group of β-carbonic anhydrases, Proc. Natl. Acad. Sci. U. S. A., 113 (2016) 14716-14721.
[95] S. He, H.-T. Chou, D. Matthies, T. Wunder, M.T. Meyer, N. Atkinson, A. Martinez-Sanchez, P.D. Jeffrey, S.A. Port, W. Patena, G. He, V.K. Chen, F.M. Hughson, A.J. McCormick, O. Mueller-Cajar, B.D. Engel, Z. Yu, M.C. Jonikas, The Structural Basis of Rubisco Phase Separation in the Pyrenoid, Nature Plants, 6 (2020) 1480-1490.
[96] T.K. Antal, I.B. Kovalenko, A.B. Rubin, E. Tyystjärvi, Photosynthesis-related quantities for education and modeling, Photosynth. Res., 117 (2013) 1-30.
[97] N. Atkinson, C.N. Velanis, T. Wunder, D.J. Clarke, O. Mueller-Cajar, A.J. McCormick, The pyrenoidal linker protein EPYC1 phase separates with hybrid Arabidopsis-Chlamydomonas Rubisco through interactions with the algal Rubisco small subunit, J. Exp. Bot., 70 (2019) 5271-5285.
[98] M.T. Meyer, T. Genkov, J.N. Skepper, J. Jouhet, M.C. Mitchell, R.J. Spreitzer, H. Griffiths, Rubisco small-subunit α-helices control pyrenoid formation in *Chlamydomonas*, Proc. Natl. Acad. Sci. U. S. A., 109 (2012) 19474-19479.
[99] J.S. MacCready, J.L. Basalla, A.G. Vecchiarelli, Origin and Evolution of Carboxysome Positioning Systems in Cyanobacteria, Mol. Biol. Evol., 37 (2020) 1434-1451.
[100] M.M.M. Goudet, D.J. Orr, M. Melkonian, K.H. Müller, M.T. Meyer, E. Carmo-Silva, H. Griffiths, Rubisco and carbon concentrating mechanism (CCM) co-evolution across Chlorophyte and Streptophyte green algae, New Phytol., 227 (2020) 810-823.
[101] M.T. Meyer, A.K. Itakura, W. Patena, L. Wang, S. He, T. Emrich-Mills, C.S. Lau, G. Yates, L.C.M. Mackinder, M.C. Jonikas, Assembly of the algal CO_2-fixing organelle, the pyrenoid, is guided by a Rubisco-binding motif, Science Advances, 6 (2020) eabd2408.
[102] E. Voronina, G. Seydoux, P. Sassone-Corsi, I. Nagamori, RNA granules in germ cells, Cold Spring Harb. Perspect. Biol., 3 (2011) a002774.
[103] M. Wilsch-Bräuninger, H. Schwarz, C. Nüsslein-Volhard, A sponge-like structure involved in the association and transport of maternal products during *Drosophila oogenesis*, J. Cell Biol., 139 (1997) 817-829.
[104] M.J. Snee, P.M. Macdonald, Dynamic organization and plasticity of sponge bodies, Dev. Dyn., 238 (2009) 918-930.
[105] X. Su, J.A. Ditlev, E. Hui, W. Xing, S. Banjade, J. Okrut, D.S. King, J. Taunton, M.K. Rosen, R.D. Vale, Phase separation of signaling molecules promotes T cell receptor signal transduction, Science, 352 (2016) 595-599.
[106] S. Banjade, M.K. Rosen, Phase transitions of multivalent proteins can promote clustering of membrane receptors, Elife, 3 (2014) e04123.

[107] H.B. Schmidt, D. Görlich, Transport Selectivity of Nuclear Pores, Phase Separation, and Membraneless Organelles, Trends Biochem. Sci., 41 (2016) 46-61.
[108] J.E. Lee, P.I. Cathey, H. Wu, R. Parker, G.K. Voeltz, Endoplasmic reticulum contact sites regulate the dynamics of membraneless organelles, Science, 367 (2020) eaay7108.
[109] W. Ma, C. Mayr, A Membraneless Organelle Associated with the Endoplasmic Reticulum Enables 3′UTR-Mediated Protein-Protein Interactions, Cell, 175 (2018) 1492-1506.e1419.
[110] Y. Fujioka, J. Alam, D. Noshiro, K. Mouri, T. Ando, Y. Okada, A.I. May, R.L. Knorr, K. Suzuki, Y. Ohsumi, N.N. Noda, Phase separation organizes the site of autophagosome formation, Nature, 578 (2020) 301-305.
[111] D. Milovanovic, Y. Wu, X. Bian, P. De Camilli, A liquid phase of synapsin and lipid vesicles, Science, 361 (2018) 604-607.
[112] W.F. Zeno, U. Baul, W.T. Snead, A.C.M. DeGroot, L. Wang, E.M. Lafer, D. Thirumalai, J.C. Stachowiak, Synergy between intrinsically disordered domains and structured proteins amplifies membrane curvature sensing, Nat. Commun., 9 (2018) 4152.
[113] W.F. Zeno, A.S. Thatte, L. Wang, W.T. Snead, E.M. Lafer, J.C. Stachowiak, Molecular Mechanisms of Membrane Curvature Sensing by a Disordered Protein, J. Am. Chem. Soc., 141 (2019) 10361-10371.
[114] L. Boudière, M. Michaud, D. Petroutsos, F. Rébeillé, D. Falconet, O. Bastien, S. Roy, G. Finazzi, N. Rolland, J. Jouhet, M.A. Block, E. Maréchal, Glycerolipids in photosynthesis: Composition, synthesis and trafficking, Biochimica et Biophysica Acta (BBA) - Bioenergetics, 1837 (2014) 470–480.
[115] H. Kirchhoff, U. Mukherjee, H.J. Galla, Molecular architecture of the thylakoid membrane: lipid diffusion space for plastoquinone, Biochemistry, 41 (2002) 4872-4882.
[116] B. Andersson, J.M. Anderson, Lateral heterogeneity in the distribution of chlorophyll-protein complexes of the thylakoid membranes of spinach chloroplasts, Biochim. Biophys. Acta, 593 (1980) 427-440.
[117] A.M. Pyszniak, S.P. Gibbs, Immunocytochemical localization of photosystem I and the fucoxanthin-chlorophylla/c light-harvesting complex in the diatom *Phaeodactylum tricornutum*, Protoplasma, 166 (1992) 208-217.
[118] I. Tsekos, F.X. Niell, J. Aguilera, F. Lopez-Figueroa, S.G. Delivopoulos, Ultrastructure of the vegetative gametophytic cells of *Porphyra leucosticta* (Rhodophyta) grown in red, blue and green light, Phycological Res., 50 (2002) 251-264.
[119] F. Yuan, H. Alimohamadi, B. Bakka, A.N. Trementozzi, N.L. Fawzi, P. Rangamani, J.C. Stachowiak, Membrane bending by protein phase separation, bioRxiv, (2020) 10.1101/2020.05.21.109751.
[120] O.D. Caspari, M.T. Meyer, D. Tolleter, T.M. Wittkopp, N.J. Cunniffe, T. Lawson, A.R. Grossman, H. Griffiths, Pyrenoid loss in *Chlamydomonas reinhardtii* causes limitations in CO_2 supply, but not thylakoid operating efficiency, J. Exp. Bot., 68 (2017) 3903-3913.
[121] A. Mechela, S. Schwenkert, J. Soll, A brief history of thylakoid biogenesis, Open Biol., 9 (2019) 180237.
[122] D.J. Griffiths, The pyrenoid, Bot. Rev., 36 (1970) 29-58.
[123] K. Chan, Ultrastructure of Pyrenoid Division in *Coelastrum* sp., Cytologia, 39 (1974) 531-536.
[124] L.R. Hoffman, Observations on the fine structure of Oedogonium. V. Evidence for the de novo Formation of Pyrenoids in Zoospores of *OE. cardiacum*, J. Phycol., 4 (1968) 212-218.
[125] B. Retallack, R.D. Butler, The development and structure of pyrenoids in *Bulbochaete hiloensis*, J. Cell Sci., 6 (1970) 229-241.
[126] T. Ohiwa, Observations on chloroplast growth and pyrenoid formation in *Spirogyra*. A study by means of uncoiled picture of chloroplast, Bot Mag Tokyo, 89 (1976) 259-266.
[127] E. Gantt, S.F. Conti, The ultrastructure of *Porphyridium cruentum*, J. Cell Biol., 26 (1965) 365-381.
[128] T. Hori, I. Inouye, The ultrastructure of mitosis in *Cricosphaera roscoffensis* var. *haptonemofera* (Prymnesiophyceae), Protoplasma, 106 (1981) 121-135.

[129] K.L. Schornstein, J. Scott, Ultrastructure of cell division in the unicellular red alga *Porphyridium purpureum*, Can. J. Bot., 60 (1982) 85-97.
[130] C.A. Lander, The Relation of the Plastid to Nuclear Division in *Anthoceros laevis*, Am. J. Bot., 22 (1935) 42-51.
[131] L.V. Evans, Distribution of pyrenoids among some brown algae, J. Cell Sci., 1 (1966) 449-454.
[132] E.J. Cox, Observations on the morphology and vegetative cell division of the diatom *Donkinia recta*, Helgoländer Meeresuntersuchungen, 34 (1981) 497-506.
[133] T. Osafune, A. Yokota, S. Sumida, E. Hase, Immunogold Localization of Ribulose-1,5-Bisphosphate Carboxylase with Reference to Pyrenoid Morphology in Chloroplasts of Synchronized *Euglena gracilis* Cells, Plant Physiol., 92 (1990) 802-808.
[134] C. Nagasato, T. Motomura, New Pyrenoid Formation in the Brown Alga, *Scytosiphon lomentaria* (Scytosiphonales, Phaeophyceae), J. Phycol., 38 (2002) 800-806.
[135] F. McAllister, The Pyrenoids of *Anthoceros* and *Notothylas* with Especial Reference to Their Presence in Spore Mother Cells, Am. J. Bot., 14 (1927) 246-257.
[136] C.N. Sun, Submicroscopic structure and development of the chloroplast and pyrenoid in *Anthoceros laevis*, Protoplasma, 55 (1962) 89-98.
[137] K. Ueda, The Pyrenoid of *Chlorogonium elongatum*, in: H. Tamiya (Ed.) Studies on Microalgae and Photosynthetic Bacteria: A Collection of Papers Dedicated to Hiroshi Tamiya on the Occasion of His 60th Birthday, Japanese Society of Plant Physiologists, University of Tokyo Press, Tokyo, 1963, pp. 636.
[138] G.M. Smith, Cytological Studies in the Protococcales. III. Cell Structure and Autospore Formation in *Tetraedron minimum* (A. Br.), Hansg, Ann. Bot., 32 (1918) 459-464.
[139] M. Vítová, J. Hendrychova, M. Čížková, V. Cepak, J.G. Umen, V. Zachleder, K. Bišová, Accumulation, activity and localization of cell cycle regulatory proteins and the chloroplast division protein FtsZ in the alga *Scenedesmus quadricauda* under inhibition of nuclear DNA replication, Plant Cell Physiol., 49 (2008) 1805-1817.
[140] K.C. Vaughn, E.O. Campbell, J. Hasegawa, H.A. Owen, K.S. Renzaglia, The pyrenoid is the site of ribulose 1,5-bisphosphate carboxylase/oxygenase accumulation in the hornwort (Bryophyta: Anthocerotae) chloroplast, Protoplasma, 156 (1990) 117-129.
[141] U.W. Goodenough, Chloroplast Division and Pyrenoid Formation in *Chlamydomonas reinhardi*, J. Phycol., 6 (1970) 1-6.
[142] I. Manton, Further observations on the fine structure of *Chrysochromulina chiton* with special reference to the haptonema, 'peculiar' golgi structure and scale production, J. Cell Sci., 2 (1967) 265-272.
[143] S. Schuette, K.S. Renzaglia, Development of multicellular spores in the hornwort genus *Dendroceros* (Dendrocerotaceae, Anthocerotophyta) and the occurrence of endospory in Bryophytes, Nova Hedwigia, 91 (2010) 301-316.
[144] R. Subrahmanyan, On the cell-division and mitosis in some South Indian diatoms, Proc. Indian Acad. Sci., 22 (1945) 331-354.
[145] D.G. Mann, In vivo Observations of Plastid and Cell Division in Raphid Diatoms and Their Relevance to Diatom Systematics, Ann. Bot., 55 (1985) 95-108.
[146] A. Tanaka, C. Nagasato, S. Uwai, T. Motomura, H. Kawai, Re-examination of ultrastructures of the stellate chloroplast organization in brown algae: Structure and development of pyrenoids, Phycological Res., 55 (2007) 203-213.
[147] L.M. Patrone, S.T. Broadwater, J.L. Scott, Ultrastructure of vegetative and dividing cells of the unicellular red algae *Rhodella violacea* and *Rhodella maculata*, J. Phycol., 27 (1991) 742-753.
[148] A. Jenks, S.P. Gibbs, Immunolocalization and distribution of form ii rubisco in the pyrenoid and chloroplast stroma of *Amphidinium carterae* and form i rubisco in the symbiont-derived plastids of *Peridinium foliaceum* (dinophyceae), J. Phycol., 36 (2000) 127-138.
[149] U.G. Johnson, K.R. Porter, Fine Structure of Cell Division in *Chlamydomonas reinhardi*: Basal Bodies and Microtubules, Journal of Cell Biology, 38 (1968) 403-425.
[150] E.T. O'Toole, S.K. Dutcher, Site-specific basal body duplication in *Chlamydomonas*, Cytoskeleton (Hoboken), 71 (2014) 108-118.

[151] S. Vitha, R.S. McAndrew, K.W. Osteryoung, FtsZ ring formation at the chloroplast division site in plants, J. Cell Biol., 153 (2001) 111-120.
[152] A.D. TerBush, Y. Yoshida, K.W. Osteryoung, FtsZ in chloroplast division: structure, function and evolution, Curr. Opin. Cell Biol., 25 (2013) 461-470.
[153] K. Kanamaru, M. Fujiwara, M. Kim, A. Nagashima, E. Nakazato, K. Tanaka, H. Takahashi, Chloroplast targeting, distribution and transcriptional fluctuation of AtMinD1, a Eubacteria-type factor critical for chloroplast division, Plant Cell Physiol., 41 (2000) 1119-1128.
[154] F. van den Ent, L. Amos, J. Löwe, Bacterial ancestry of actin and tubulin, Curr. Opin. Microbiol., 4 (2001) 634-638.
[155] T. Wakasugi, T. Nagai, M. Kapoor, M. Sugita, M. Ito, S. Ito, J. Tsudzuki, K. Nakashima, T. Tsudzuki, Y. Suzuki, A. Hamada, T. Ohta, A. Inamura, K. Yoshinaga, M. Sugiura, Complete nucleotide sequence of the chloroplast genome from the green alga *Chlorella vulgaris*: the existence of genes possibly involved in chloroplast division, Proc. Natl. Acad. Sci. U. S. A., 94 (1997) 5967-5972.
[156] Y. Hu, Z.-W. Chen, W.-Z. Liu, X.-L. Liu, Y.-K. He, Chloroplast division is regulated by the circadian expression of FTSZ and MIN genes in *Chlamydomonas reinhardtii*, Eur. J. Phycol., 43 (2008) 207-215.
[157] Y. Hirakawa, K.-I. Ishida, Prospective function of FtsZ proteins in the secondary plastid of chlorarachniophyte algae, BMC Plant Biol., 15 (2015) 276.
[158] B.T. Hovde, C. Deodato, R.A. Andersen, S. Starkenburg, R.A. Cattolico, others, *Chrysochromulina*: Genomic assessment and taxonomic diagnosis of the type species for an oleaginous algal clade, Algal Res, 37 (2019) 307-319.
[159] S.-Y. Miyagishima, K. Suzuki, K. Okazaki, Y. Kabeya, Expression of the nucleus-encoded chloroplast division genes and proteins regulated by the algal cell cycle, Mol. Biol. Evol., 29 (2012) 2957-2970.
[160] R. Onuma, N. Mishra, S.-Y. Miyagishima, Regulation of chloroplast and nucleomorph replication by the cell cycle in the cryptophyte *Guillardia theta*, Sci. Rep., 7 (2017) 2345.
[161] D.C. Price, U.W. Goodenough, R. Roth, J.-H. Lee, T. Kariyawasam, M. Mutwil, C. Ferrari, F. Facchinelli, S.G. Ball, U. Cenci, C.X. Chan, N.E. Wagner, H.S. Yoon, A.P.M. Weber, D. Bhattacharya, Analysis of an improved *Cyanophora paradoxa* genome assembly, DNA Res., 26 (2019) 287-299.
[162] N. Sumiya, A. Hirata, S. Kawano, Multiple FtsZ Ring Formation and Reduplicated Chlorplast DNA in *Nannochloris bacillaris* (Chlorophyta, Trebouxiophyceae) Under Phosphate-enriched Culture, J. Phycol., 44 (2008) 1476-1489.
[163] N. Sumiya, S. Owari, K. Watanabe, S. Kawano, Role of Multiple FtsZ Rings in Chloroplast Division Under Oligotrophic and Eutrophic Conditions in the Unicellular Green Algal *Nannochloris bacillaris* (Chlorophyta, Trebouxiophyceae), J. Phycol., 48 (2012) 1187-1196.
[164] M. Onishi, J.G. Umen, F.R. Cross, J.R. Pringle, Cleavage-furrow formation without F-actin in *Chlamydomonas*, Proc. Natl. Acad. Sci. U. S. A., (2020).
[165] T. Mita, T. Kuroiwa, Division of Plastids by a Plastid-Dividing Ring in *Cyanidium caldarium*, in: M. Tazawa (Ed.) Cell Dynamics: Cytoplasmic Streaming Cell Movement—Contraction and Migration Cell and Organelle Division Phototaxis of Cell and Cell Organelle, Springer Vienna, Place Published, 1989, pp. 133-152.
[166] H. Hashimoto, Involvement of actin filaments in chloroplast division of the alga *Closterium ehrenbergii*, Protoplasma, 167 (1992) 88-96.
[167] J.D. Harper, D.W. McCurdy, M.A. Sanders, J.L. Salisbury, P.C. John, Actin dynamics during the cell cycle in *Chlamydomonas reinhardtii*, Cell Motil. Cytoskeleton, 22 (1992) 117-126.
[168] G.O. Wasteneys, D.A. Collings, B.E.S. Gunning, P.K. Hepler, D. Menzel, Actin in living and fixed characean internodal cells: identification of a cortical array of fine actin strands and chloroplast actin rings, Protoplasma, 190 (1996) 25-38.
[169] D.E. Wujek, K.E. Camburn, H.T. Andrews, An ultrastructural study of pyrenoids in *Leptosiropsis torulosa*, Protoplasma, 86 (1975) 263-268.

[170] G.M. Lokhorst, W. Star, Pyrenoid Ultrastructure in *Ulothrix* (Chlorophyceae), Acta Bot. Neerl., 29 (1980) 1-15.
[171] A. Giustiniani, W. Drenckhan, C. Poulard, Interfacial tension of reactive, liquid interfaces and its consequences, Adv. Colloid Interface Sci., 247 (2017) 185-197.
[172] R.M. Brown, H.C. Bold, R.N. Lester, Comparative studies of the algal genera *Tetracystis* and *Chlorococcum*, University of Texas, Place Published, 1964.
[173] F. McAllister, The Pyrenoid of *Anthoceros*, Am. J. Bot., 1 (1914) 79-95.
[174] T. Bisalputra, T.E. Weier, The pyrenoid of *Scenedesmus quadricauda*, Am. J. Bot., 51 (1964) 881-892.
[175] M. Hofweber, D. Dormann, Friend or foe—Post-translational modifications as regulators of phase separation and RNP granule dynamics, J. Biol. Chem., 294 (2019) 7137-7150.
[176] A. Bah, J.D. Forman-Kay, Modulation of Intrinsically Disordered Protein Function by Post-translational Modifications, J. Biol. Chem., 291 (2016) 6696-6705.
[177] A. Wang, A.E. Conicella, H.B. Schmidt, E.W. Martin, S.N. Rhoads, A.N. Reeb, A. Nourse, D. Ramirez Montero, V.H. Ryan, R. Rohatgi, Others, A single N-terminal phosphomimic disrupts TDP-43 polymerization, phase separation, and RNA splicing, EMBO J., 37 (2018) e97452.
[178] J. Söding, D. Zwicker, S. Sohrabi-Jahromi, M. Boehning, J. Kirschbaum, Mechanisms for Active Regulation of Biomolecular Condensates, Trends in Cell Biology, 30 (2020) 4-14.
[179] D. Zwicker, R. Seyboldt, C.A. Weber, A.A. Hyman, F. Jülicher, Growth and division of active droplets provides a model for protocells, Nat. Phys., 13 (2017) 408-413.
[180] M.V. Turkina, A. Blanco-Rivero, J.P. Vainonen, A.V. Vener, A. Villarejo, CO_2 limitation induces specific redox-dependent protein phosphorylation in *Chlamydomonas reinhardtii*, Proteomics, 6 (2006) 2693-2704.
[181] H. Wang, B. Gau, W.O. Slade, M. Juergens, P. Li, L.M. Hicks, The global phosphoproteome of *Chlamydomonas reinhardtii* reveals complex organellar phosphorylation in the flagella and thylakoid membrane, Mol. Cell. Proteomics, 13 (2014) 2337-2353.
[182] E.P. Bentley, B.B. Frey, A.A. Deniz, Physical Chemistry of Cellular Liquid-Phase Separation, Chem. Eur. J., 25 (2019) 5600-5610.
[183] T. Wunder, Z.G. Oh, O. Mueller-Cajar, CO_2-fixing liquid droplets: towards a dissection of the microalgal pyrenoid, Traffic, 20 (2019) 380-389.
[184] K.L. Pennington, T.Y. Chan, M.P. Torres, J.L. Andersen, The dynamic and stress-adaptive signaling hub of 14-3-3: emerging mechanisms of regulation and context-dependent protein–protein interactions, Oncogene, 37 (2018) 5587-5604.
[185] T. Obsil, V. Obsilova, Structural basis of 14-3-3 protein functions, Semin. Cell Dev. Biol., 22 (2011) 663-672.
[186] A. Aitken, 14-3-3 proteins: a historic overview, Semin. Cancer Biol., 16 (2006) 162-172.
[187] C.W. Pak, M. Kosno, A.S. Holehouse, S.B. Padrick, A. Mittal, R. Ali, A.A. Yunus, D.R. Liu, R.V. Pappu, M.K. Rosen, Sequence Determinants of Intracellular Phase Separation by Complex Coacervation of a Disordered Protein, Mol. Cell, 63 (2016) 72-85.
[188] B. Van Treeck, D.S.W. Protter, T. Matheny, A. Khong, C.D. Link, R. Parker, RNA self-assembly contributes to stress granule formation and defining the stress granule transcriptome, Proc. Natl. Acad. Sci. U. S. A., 115 (2018) 2734-2739.
[189] Y. Ma, S.V. Pollock, Y. Xiao, K. Cunnusamy, J.V. Moroney, Identification of a novel gene, CIA6, required for normal pyrenoid formation in *Chlamydomonas reinhardtii*, Plant Physiol., 156 (2011) 884-896.
[190] A.J. Brueggeman, D.S. Gangadharaiah, M.F. Cserhati, D. Casero, D.P. Weeks, I. Ladunga, Activation of the carbon concentrating mechanism by CO_2 deprivation coincides with massive transcriptional restructuring in *Chlamydomonas reinhardtii*, Plant Cell, 24 (2012) 1860-1875.
[191] W. Fang, Y. Si, S. Douglass, D. Casero, S.S. Merchant, M. Pellegrini, I. Ladunga, P. Liu, M.H. Spalding, Transcriptome-wide changes in *Chlamydomonas reinhardtii* gene

expression regulated by carbon dioxide and the CO_2-concentrating mechanism regulator CIA5/CCM1, Plant Cell, 24 (2012) 1876-1893.
[192] P. Cloutier, M. Lavallée-Adam, D. Faubert, M. Blanchette, B. Coulombe, A newly uncovered group of distantly related lysine methyltransferases preferentially interact with molecular chaperones to regulate their activity, PLoS Genet., 9 (2013) e1003210.
[193] O.N. Borkhsenious, C.B. Mason, J.V. Moroney, The intracellular localization of ribulose-1,5-bisphosphate Carboxylase/Oxygenase in *Chlamydomonas reinhardtii*, Plant Physiol., 116 (1998) 1585-1591.
[194] M.C. Mitchell, M.T. Meyer, H. Griffiths, Dynamics of carbon-concentrating mechanism induction and protein relocalization during the dark-to-light transition in synchronized *Chlamydomonas reinhardtii*, Plant Physiol., 166 (2014) 1073-1082.
[195] M.C. Munder, D. Midtvedt, T. Franzmann, E. Nüske, O. Otto, M. Herbig, E. Ulbricht, P. Müller, A. Taubenberger, S. Maharana, L. Malinovska, D. Richter, J. Guck, V. Zaburdaev, S. Alberti, A pH-driven transition of the cytoplasm from a fluid- to a solid-like state promotes entry into dormancy, Elife, 5 (2016) e09347.
[196] T.M. Franzmann, M. Jahnel, A. Pozniakovsky, J. Mahamid, A.S. Holehouse, E. Nüske, D. Richter, W. Baumeister, S.W. Grill, R.V. Pappu, A.A. Hyman, S. Alberti, Phase separation of a yeast prion protein promotes cellular fitness, Science, 359 (2018) eaao5654.
[197] T.J. Nott, E. Petsalaki, P. Farber, D. Jervis, E. Fussner, A. Plochowietz, T.D. Craggs, D.P. Bazett-Jones, T. Pawson, J.D. Forman-Kay, A.J. Baldwin, Phase transition of a disordered nuage protein generates environmentally responsive membraneless organelles, Mol. Cell, 57 (2015) 936-947.
[198] J.A. Riback, C.D. Katanski, J.L. Kear-Scott, E.V. Pilipenko, A.E. Rojek, T.R. Sosnick, D.A. Drummond, Stress-Triggered Phase Separation Is an Adaptive, Evolutionarily Tuned Response, Cell, 168 (2017) 1028-1040.e1019.
[199] K. Oglęcka, P. Rangamani, B. Liedberg, R.S. Kraut, A.N. Parikh, Oscillatory phase separation in giant lipid vesicles induced by transmembrane osmotic differentials, Elife, 3 (2014) e03695.
[200] J.V. Moroney, R.A. Ynalvez, Proposed carbon dioxide concentrating mechanism in *Chlamydomonas reinhardtii*, Eukaryot. Cell, 6 (2007) 1251-1259.
[201] J.H. Hennacy, M.C. Jonikas, Prospects for Engineering Biophysical CO_2 Concentrating Mechanisms into Land Plants to Enhance Yields, Annu. Rev. Plant Biol., 71 (2020) 461-485.
[202] S. Kroschwald, M.C. Munder, S. Maharana, T.M. Franzmann, D. Richter, M. Ruer, A.A. Hyman, S. Alberti, Different Material States of Pub1 Condensates Define Distinct Modes of Stress Adaptation and Recovery, Cell Rep., 23 (2018) 3327-3339.
[203] T.K. Harris, G.J. Turner, Structural basis of perturbed pKa values of catalytic groups in enzyme active sites, IUBMB Life, 53 (2002) 85-98.
[204] M. Vítová, K. Bišová, M. Hlavová, S. Kawano, V. Zachleder, M. Cížková, *Chlamydomonas reinhardtii*: duration of its cell cycle and phases at growth rates affected by temperature, Planta, 234 (2011) 599-608.
[205] R.M. Morgan-Kiss, A.G. Ivanov, S. Modla, K. Czymmek, N.P.A. Hüner, J.C. Priscu, J.T. Lisle, T.E. Hanson, Identity and physiology of a new psychrophilic eukaryotic green alga, *Chlorella* sp., strain BI, isolated from a transitory pond near Bratina Island, Antarctica, Extremophiles, 12 (2008) 701-711.
[206] B. Eddie, C. Krembs, S. Neuer, Characterization and growth response to temperature and salinity of psychrophilic, halotolerant *Chlamydomonas* sp. ARC isolated from Chukchi Sea ice, Mar. Ecol. Prog. Ser., 354 (2008) 107-117.
[207] S. Yau, A. Lopes Dos Santos, W. Eikrem, C. Gérikas Ribeiro, P. Gourvil, S. Balzano, M.-L. Escande, H. Moreau, D. Vaulot, *Mantoniella beaufortii* and *Mantoniella baffinensis* sp. nov. (Mamiellales, Mamiellophyceae), two new green algal species from the high arctic, J. Phycol., 56 (2020) 37-51.
[208] A. Kremp, M. Elbrächter, M. Schweikert, J.L. Wolny, M. Gottschling, *Woloszynskia halophila* (Biecheler) comb. nov.: A Bloom-forming Cold-water Dinoflagellate Co-occurring with *Scrippsiella hangoei* (Dinophyceae) in the Baltic Sea, J. Phycol., 41 (2005) 629-642.

[209] T. Horiguchi, M. Hoppenrath, *Haramonas viridis* sp. nov. (Raphidophyceae, Heterokontophyta), a new sand-dwelling raphidophyte from cold temperate waters, Phycological Res., 51 (2003) 61-67.
[210] M. Cvetkovska, N.P.A. Hüner, D.R. Smith, Chilling out: the evolution and diversification of psychrophilic algae with a focus on *Chlamydomonadales*, Polar Biol., 40 (2017) 1169-1184.
[211] B. Szyszka-Mroz, M. Cvetkovska, A.G. Ivanov, D.R. Smith, M. Possmayer, D.P. Maxwell, N.P.A. Hüner, Cold-Adapted Protein Kinases and Thylakoid Remodeling Impact Energy Distribution in an Antarctic Psychrophile, Plant Physiol., 180 (2019) 1291-1309.
[212] L. Valledor, T. Furuhashi, A.-M. Hanak, W. Weckwerth, Systemic cold stress adaptation of *Chlamydomonas reinhardtii*, Mol. Cell. Proteomics, 12 (2013) 2032-2047.
[213] A. Patel, L. Malinovska, S. Saha, J. Wang, S. Alberti, Y. Krishnan, A.A. Hyman, ATP as a biological hydrotrope, Science, 356 (2017) 753-756.
[214] S.V. Pollock, S.L. Colombo, D.L. Prout, A.C. Godfrey, J.V. Moroney, Rubisco Activase Is Required for Optimal Photosynthesis in the Green Alga *Chlamydomonas reinhardtii* in a Low-CO_2 Atmosphere, Plant Physiol., 133 (2003) 1854-1861.
[215] O. Mueller-Cajar, The Diverse AAA+ Machines that Repair Inhibited Rubisco Active Sites, Front Mol Biosci, 4 (2017) 31.
[216] W. Yamori, C. Masumoto, H. Fukayama, A. Makino, Rubisco activase is a key regulator of non-steady-state photosynthesis at any leaf temperature and, to a lesser extent, of steady-state photosynthesis at high temperature, The Plant Journal, 71 (2012) 871-880.
[217] R.M.L. McKay, S.P. Gibbs, K.C. Vaughn, RuBisCo activase is present in the pyrenoid of green algae, Protoplasma, 162 (1991) 38-45.
[218] L. Wang, T. Yamano, S. Takane, Y. Niikawa, C. Toyokawa, S.-I. Ozawa, R. Tokutsu, Y. Takahashi, J. Minagawa, Y. Kanesaki, H. Yoshikawa, H. Fukuzawa, Chloroplast-mediated regulation of CO_2-concentrating mechanism by Ca2+-binding protein CAS in the green alga *Chlamydomonas reinhardtii*, Proc. Natl. Acad. Sci. U. S. A., 113 (2016) 12586-12591.
[219] T. Yamano, C. Toyokawa, H. Fukuzawa, High-resolution suborganellar localization of Ca2+-binding protein CAS, a novel regulator of CO_2-concentrating mechanism, Protoplasma, 255 (2018) 1015-1022.
[220] B. Liu, B. Poolman, A.J. Boersma, Ionic Strength Sensing in Living Cells, ACS Chem. Biol., 12 (2017) 2510-2514.
[221] L. Wang, T. Yamano, M. Kajikawa, M. Hirono, H. Fukuzawa, Isolation and characterization of novel high-CO_2-requiring mutants of *Chlamydomonas reinhardtii*, Photosynth. Res., 121 (2014) 175-184.
[222] L. Teng, L. Ding, Q. Lu, Microscopic observation of pyrenoids in order Ulvales (Chlorophyta) collected from Qingdao coast, J. Ocean Univ. China, 10 (2011) 223-228.
[223] I. Dehning, M.M. Tilzer, Survival of *Scenedesmus acuminatus* (Chlorophyceaea) in Darkness, J. Phycol., 25 (1989) 509-515.
[224] P.W. Voorhees, The theory of Ostwald ripening, J. Stat. Phys., 38 (1985) 231-252.
[225] Y. Shin, Y.-C. Chang, D.S.W. Lee, J. Berry, D.W. Sanders, P. Ronceray, N.S. Wingreen, M. Haataja, C.P. Brangwynne, Liquid Nuclear Condensates Mechanically Sense and Restructure the Genome, Cell, 175 (2018) 1481-1491.e1413.
[226] M.C. Mitchell, G. Metodieva, M.V. Metodiev, H. Griffiths, M.T. Meyer, Pyrenoid loss impairs carbon-concentrating mechanism induction and alters primary metabolism in *Chlamydomonas reinhardtii*, J. Exp. Bot., 68 (2017) 3891-3902.
[227] R.J. Blank, R.K. Trench, Immunogold localization of Ribulose-1.5-bisphosphate carboxylase-oxygenase in *Symbiodinium kawahutii* trench et blank - An Endosymbiotic Dinoflagellate, Endocytobiosis Cell Res., 5 (1988) 75-82.
[228] H. Kajikawa, M. Okada, F. Ishikawa, Y. Okada, K. Nakayama, Immunochemical Studies on Ribulose 1,5-Bisphosphate Carboxylase/Oxygenase in the Chloroplasts of the Marine Alga *Bryopsis maxima*, Plant Cell Physiol., 29 (1988) 549-556.
[229] J.Z. Kiss, A.C. Vasoconcelos, R.E. Triemer, Paramylon Synthesis and Chloroplast Structure Associated with Nutrient Levels in *Euglena* (Euglenophyceae), J. Phycol., 22 (1986) 327-333.

[230] R.M.L. McKay, S.P. Gibbs, Immunocytochemical localization of ribulose 1,5-bisphosphate carboxylase/oxygenase in light-limited and light-saturated cells of *Chlorella pyrenoidosa*, Protoplasma, 149 (1989) 31-37.
[231] L. Mustardy, F.X. Cunningham, E. Gantt, Localization and quantitation of chloroplast enzymes and light-harvesting components using immunocytochemical methods, Plant Physiol., 94 (1990) 334-340.
[232] T. Osafune, S. Sumida, T. Ehara, E. Hase, Three-Dimensional Distribution of Ribulose-1,5-Bisphosphate Carboxylase/Oxygenase in Chloroplasts of Actively Photosynthesizing Cell of *Euglena gracilis*, J. Electron Microsc., 38 (1989) 399-402.
[233] N. Nassoury, L. Fritz, D. Morse, Circadian changes in ribulose-1,5-bisphosphate carboxylase/oxygenase distribution inside individual chloroplasts can account for the rhythm in dinoflagellate carbon fixation, Plant Cell, 13 (2001) 923-934.
[234] S. Lin, E.J. Carpenter, Rubisco of *Dunaliella tertiolecta* is redistributed between the pyrenoid and the stroma as a light /shade response, Mar. Biol., 127 (1997) 521-529.
[235] J.A. Raven, M. Giordano, J. Beardall, S.C. Maberly, Algal evolution in relation to atmospheric CO_2: carboxylases, carbon-concentrating mechanisms and carbon oxidation cycles, Philos. Trans. R. Soc. Lond. B Biol. Sci., 367 (2012) 493-507.
[236] E. Morita, M. Abe T Fau - Tsuzuki, S. Tsuzuki M Fau - Fujiwara, N. Fujiwara S Fau - Sato, A. Sato N Fau - Hirata, K. Hirata A Fau - Sonoike, H. Sonoike K Fau - Nozaki, H. Nozaki, Presence of the CO_2-concentrating mechanism in some species of the pyrenoid-less free-living algal genus *Chloromonas* (Volvocales, Chlorophyta), Planta, 204 (1998) 269-276.
[237] J.C. Villarreal, K.S. Renzaglia, The hornworts: important advancements in early land plant evolution, J. Bryol., 37 (2015) 157-170.
[238] A. Flamholz, P.M. Shih, Cell biology of photosynthesis over geologic time, Curr. Biol., 30 (2020) R490-R494.
[239] J. Zhang, X.-X. Fu, R.-Q. Li, X. Zhao, Y. Liu, M.-H. Li, A. Zwaenepoel, H. Ma, B. Goffinet, Y.-L. Guan, J.-Y. Xue, Y.-Y. Liao, Q.-F. Wang, Q.-H. Wang, J.-Y. Wang, G.-Q. Zhang, Z.-W. Wang, Y. Jia, M.-Z. Wang, S.-S. Dong, J.-F. Yang, Y.-N. Jiao, Y.-L. Guo, H.-Z. Kong, A.-M. Lu, H.-M. Yang, S.-Z. Zhang, Y. Van de Peer, Z.-J. Liu, Z.-D. Chen, The hornwort genome and early land plant evolution, Nat Plants, 6 (2020) 107-118.
[240] V. Ahmadjian, Trebouxia: Reflections on a Perplexing and Controversial Lichen Photobiont, in: J. Seckbach (Ed.) Symbiosis: Mechanisms and Model Systems, Springer Netherlands, Place Published, 2002, pp. 373-383.
[241] L.R. Hoffman, Observations on the Fine Structure of *Oedogonium* IV. The Mature Pyrenoid of *Oe. cardiacum*, Trans. Am. Microsc. Soc., 87 (1968) 178-185.
[242] S.P. Gibbs, The ultrastructure of the pyrenoids of green algae, J. Ultrastruct. Res., 7 (1962) 262-272.
[243] G.M. Lokhorst, H.J. Sluiman, W. Star, The Ultrastructure of Mitosis and Cytokinesis in the Sarcinoid *Chlorokybus atmophticus* (Chlorophyta, Charophyceae) Revealed by Rapid Freeze Fixation and Freeze Substitution, J. Phycol., 24 (1988) 237-248.
[244] S. Kikutani, K. Nakajima, C. Nagasato, Y. Tsuji, A. Miyatake, Y. Matsuda, Thylakoid luminal θ-carbonic anhydrase critical for growth and photosynthesis in the marine diatom *Phaeodactylum tricornutum*, Proc. Natl. Acad. Sci. U. S. A., 113 (2016) 9828-9833.
[245] H.E. Calvert, C.J. Dawes, M.A. Borowitzka, Phlylogenetic relationships of *Caulerpa* (Chlorophyta) based on comparative ultrastructure, J. Phycol., 12 (1976) 149-162.
[246] J. Scott, E.-C. Yang, J.A. West, A. Yokoyama, H.-J. Kim, S.L. De Goer, C.J. O'Kelly, E. Orlova, S.-Y. Kim, J.-K. Park, Others, On the genus Rhodella, the emended orders Dixoniellales and Rhodellales with a new order Glaucosphaerales (Rhodellophyceae, Rhodophyta), Algae, 26 (2011) 277-288.
[247] T. Mikhailyuk, A. Lukešová, K. Glaser, A. Holzinger, S. Obwegeser, S. Nyporko, T. Friedl, U. Karsten, New Taxa of Streptophyte Algae (Streptophyta) from Terrestrial Habitats Revealed Using an Integrative Approach, Protist, 169 (2018) 406-431.
[248] Y.D. Bedoshvili, T.P. Popkova, Y.V. Likhoshway, Chloroplast structure of diatoms of different classes, Cell tissue biol., 3 (2009) 297-310.

[249] A. De Martino, A. Bartual, A. Willis, A. Meichenin, B. Villazán, U. Maheswari, C. Bowler, Physiological and molecular evidence that environmental changes elicit morphological interconversion in the model diatom *Phaeodactylum tricornutum*, Protist, 162 (2011) 462-481.
[250] K.L. McDonald, J.D. Pickett-Heaps, Ultrastructure and differentiation in *Cladophora glomerata*. I. Cell division., Am. J. Bot., 63 (1976) 592-601.
[251] K.-I. Ishida, N. Ishida, Y. Hara, *Lotharella amoeboformis* sp. nov.: A new species of chlorarachniophytes from Japan, Phycological Res., 48 (2000) 221-229.
[252] S.Y. Lee, H.J. Jeong, N.S. Kang, T.Y. Jang, S.H. Jang, T.C. Lajeunesse, *Symbiodinium tridacnidorum* sp. nov., a dinoflagellate common to Indo-Pacific giant clams, and a revised morphological description of *Symbiodinium microadriaticum* Freudenthal, emended Trench & Blank, Eur. J. Phycol., 50 (2015) 155-172.
[253] J.D. Dodge, The Fine Structure of Chloroplasts and Pyrenoids in Some Marine Dinoflagellates, Journal of Cell Science, 3 (1968) 41.
[254] J. Deane, D. Hill, S. Brett, G. McFadden, *Hanusia phi* gen. et sp. nov. (Cryptophyceae): characterization of '*Cryptomonas* sp. Φ', Eur. J. Phycol., 33 (1998) 149-154.
[255] J. Fresnel, I. Probert, The ultrastructure and life cycle of the coastal coccolithophorid *Ochrosphaera neapolitana* (Prymnesiophyceae), Eur. J. Phycol., 40 (2005) 105-122.
[256] S. Klöpper, U. John, A. Zingone, O. Mangoni, W.H.C.F. Kooistra, A.D. Cembella, Phylogeny and morphology of a *Chattonella* (Raphidophyceae) species from the Mediterranean Sea: what is *C. subsalsa*?, Eur. J. Phycol., 48 (2013) 79-92.
[257] J.L. Scott, B. Baca, F.D. Ott, J.A. West, Light and Electron Microscopic Observations on *Erythrolobus coxiae* gen. et sp. nov.(Porphyridiophyceae, Rhodophyta) from Texas USA, Algae, 21 (2006) 407-416.
[258] F. Jouenne, W. Eikrem, F. Le Gall, D. Marie, G. Johnsen, D. Vaulot, *Prasinoderma singularis* sp. nov. (Prasinophyceae, Chlorophyta), a solitary coccoid Prasinophyte from the South-East Pacific Ocean, Protist, 162 (2011) 70-84.
[259] J.D. Dodge, The fine structure of chloroplasts and pyrenoids in some marine dinoflagellates, J. Cell Sci., 3 (1968) 41-47.
[260] S. Flori, P.-H. Jouneau, G. Finazzi, E. Maréchal, D. Falconet, Ultrastructure of the Periplastidial Compartment of the Diatom *Phaeodactylum tricornutum*, Protist, 167 (2016) 254-267.
[261] T. Hori, Comparative Studies of Pyrenoid Ultrastructure in algae of the *Monostroma Complex*, J. Phycol., 9 (1973) 190-199.
[262] J.D. Dodge, The Fine Structure of Algal Cells, Acadmeic Press, Place Published, 1973.
[263] E. Kusel-Fetzmann, M. Weidinger, Ultrastructure of five *Euglena* species positioned in the subdivision Serpentes, Protoplasma, 233 (2008) 209-222.
[264] M.E. Bakker, G.M. Lokhorst, Ultrastructure of mitosis and cytokinesis in *Zygnema* sp. (Zygnematales, Chlorophyta), Protoplasma, 138 (1987) 105-118.
[265] T. Zhan, W. Lv, Y. Deng, Multilayer gyroid cubic membrane organization in green alga *Zygnema*, Protoplasma, 254 (2017) 1923-1930.
[266] K. Trumhová, A. Holzinger, S. Obwegeser, G. Neuner, M. Pichrtová, The conjugating green alga *Zygnema* sp. (Zygnematophyceae) from the Arctic shows high frost tolerance in mature cells (pre-akinetes), Protoplasma, 256 (2019) 1681-1694.
[267] L. Van Thinh, D.J. Griffiths, H. Winsor, Ultrastructure of *Symbiodinium microadriaticum* (Dinophyceae) symbiotic with *Zoanthus sp.* (Zoanthidea), Phycologia, 25 (1986) 178-184.
[268] M. Oborník, M. Vancová, D.-H. Lai, J. Janouškovec, P.J. Keeling, J. Lukeš, Morphology and ultrastructure of multiple life cycle stages of the photosynthetic relative of apicomplexa, *Chromera velia*, Protist, 162 (2011) 115-130.
[269] G. Gärtner, B. Uzunov, E. Ingolic, W. Kofler, G. Gacheva, P. Pilarski, L. Zagorchev, M. Odjakova, M. Stoyneva, Microscopic investigations (LM, TEM and SEM) and identification of *Chlorella* isolate R-06/2 from extreme habitat in Bulgaria with a strong biological activity and resistance to environmental stress factors, Biotechnol. Biotechnol. Equip., 29 (2015) 536-540.

[270] T. Mikhailyuk, A. Holzinger, A. Massalski, U. Karsten, Morphology and ultrastructure of Interfilum and *Klebsormidium* (Klebsormidiales, Streptophyta) with special reference to cell division and thallus formation, Eur. J. Phycol., 49 (2014) 395-412.
[271] E.A. Ainsworth, S.P. Long, What have we learned from 15 years of free-air CO_2 enrichment (FACE)? A meta-analytic review of the responses of photosynthesis, canopy properties and plant production to rising CO_2, New Phytol., 165 (2005) 351-372.
[272] X.-G. Zhu, S.P. Long, D.R. Ort, What is the maximum efficiency with which photosynthesis can convert solar energy into biomass?, Curr. Opin. Biotechnol., 19 (2008) 153-159.
[273] L.C.M. Mackinder, The *Chlamydomonas* CO_2-concentrating mechanism and its potential for engineering photosynthesis in plants, New Phytol., 217 (2018) 54-61.
[274] B.D. Rae, B.M. Long, B. Förster, N.D. Nguyen, C.N. Velanis, N. Atkinson, W.Y. Hee, B. Mukherjee, G.D. Price, A.J. McCormick, Progress and challenges of engineering a biophysical carbon dioxide-concentrating mechanism into higher plants, J. Exp. Bot., 68 (2017) 3717-3737.
[275] M.T. Meyer, A.J. McCormick, H. Griffiths, Will an algal CO_2-concentrating mechanism work in higher plants?, Curr. Opin. Plant Biol., 31 (2016) 181-188.
[276] J.M. McGrath, S.P. Long, Can the Cyanobacterial Carbon-Concentrating Mechanism Increase Photosynthesis in Crop Species? A Theoretical Analysis, Plant Physiology, 164 (2014) 2247.
[277] A. Wu, G.L. Hammer, A. Doherty, S. von Caemmerer, G.D. Farquhar, Quantifying impacts of enhancing photosynthesis on crop yield, Nature Plants, 5 (2019) 380-388.
[278] P.F. South, A.P. Cavanagh, H.W. Liu, D.R. Ort, Synthetic glycolate metabolism pathways stimulate crop growth and productivity in the field, Science, 363 (2019) eaat9077.
[279] J. Kromdijk, K. Głowacka, L. Leonelli, S.T. Gabilly, M. Iwai, K.K. Niyogi, S.P. Long, Improving photosynthesis and crop productivity by accelerating recovery from photoprotection, Science, 354 (2016) 857.
[280] P.E. López-Calcagno, K.L. Brown, A.J. Simkin, S.J. Fisk, S. Vialet-Chabrand, T. Lawson, C.A. Raines, Stimulating photosynthetic processes increases productivity and water-use efficiency in the field, Nature Plants, 6 (2020) 1054-1063.
[281] N. Atkinson, D. Feike, L.C.M. Mackinder, M.T. Meyer, H. Griffiths, M.C. Jonikas, A.M. Smith, A.J. McCormick, Introducing an algal carbon-concentrating mechanism into higher plants: location and incorporation of key components, Plant Biotechnol. J., 14 (2016) 1302–1315.
[282] N. Atkinson, N. Leitão, D.J. Orr, M.T. Meyer, E. Carmo-Silva, H. Griffiths, A.M. Smith, A.J. McCormick, Rubisco small subunits from the unicellular green alga *Chlamydomonas* complement Rubisco-deficient mutants of *Arabidopsis*, New Phytol., 214 (2017) 655-667.
[283] N. Atkinson, Y. Mao, K.X. Chan, A.J. McCormick, Condensation of Rubisco into a proto-pyrenoid in higher plant chloroplasts, Nature Communications, 11 (2020) 6303.
[284] B.M. Long, W.Y. Hee, R.E. Sharwood, B.D. Rae, S. Kaines, Y.-L. Lim, N.D. Nguyen, B. Massey, S. Bala, S. von Caemmerer, M.R. Badger, G.D. Price, Carboxysome encapsulation of the CO_2-fixing enzyme Rubisco in tobacco chloroplasts, Nat. Commun., 9 (2018) 3570.